EUROPEAN ORGANIZATION FOR NUCLEAR RESEARCH

CERN-ACC-NOTE-2020-068

NIMMS-NOTE 001

COMPARISON OF ACCELERATOR DESIGNS FOR AN ION THERAPY AND RESEARCH FACILITY

E. Benedetto[1,2], U. Amaldi[2], V, Bencini[1], M. Dosanjh[1,3], P. Foka[4], D. Kaprinis[5], M. Khalvati[1], A. Lombardi[1], M. Sapinski[1,4], M. Vretenar[1], X. Zhang[6]

[1]CERN, [2]TERA Foundation, [3]Oxford University, [4]GSI, [5]Kaprinis Architect, [6]U. Melbourne

Geneva, Switzerland

December 2020

Contents

1. Introduction

1.1 New perspectives for hadron therapy

Radiotherapy or Radiation Therapy (RT) is a fundamental component of effective cancer treatment which makes use of the properties of ionizing radiation to control or kill malignant cells. It is estimated that about half of the cancer patients would benefit from radiotherapy treatment.

Radiation therapy with charged particles, such as protons and other ions species, known also as hadron therapy (HT), offers several advantages over the classical RT with X-rays. Not only do particles deposit most of their energy at the end of their penetration range, but also the charged particle beam can be shaped with great precision. This allows for more accurate tumour treatment, destroying the cancer cells more precisely with minimal damage to surrounding tissues.

The use of protons and heavier ions, such as carbon, for cancer treatment was proposed by R.R. Wilson back in 1946 [1]. In his seminal paper, he foresaw that heavy charged particles could provide utmost tumour-dose conformality and optimal sparing of surrounding critical organs and normal tissue, owing to their ability to deposit a large amount of energy at a well-localised depth depending on their energy, corresponding to the so-called Bragg peak (Figure 1). Modulating the particle energy during treatment one can vary their end of range and hence deposit their energy in the whole tumour volume (spread-out Bragg peak) as shown in Figure 1. In comparison, the traditional X-ray RT deposit more energy in the healthy tissues they traverse before and after the tumour, as shown in Figure 1 (b).

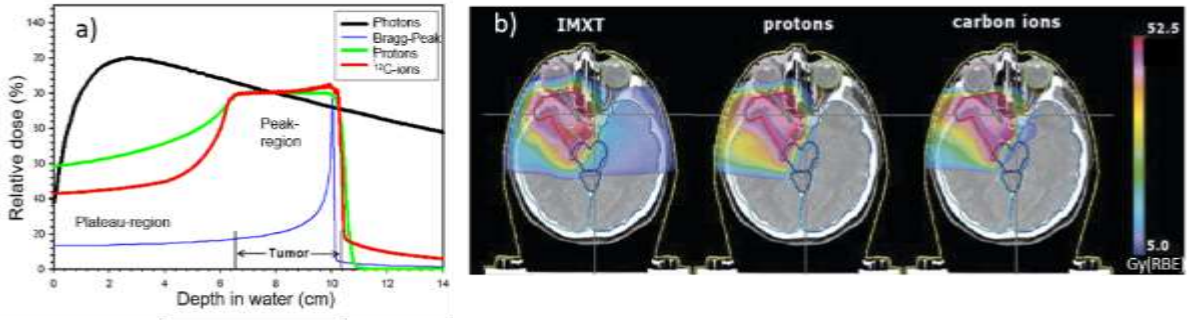

Figure 1: (left) Depth dose profiles in water and (right) treatment plans, Figure from [2] comparing photons, delivered with the most advanced intensity modulation RT (IMRT), and state-of-the-art scanned protons and ^{12}C ions, showing the increased tumour-dose conformity of ion therapy due to the characteristic Bragg peak.

Now, more than 70 years after the initial idea of using proton and heavier ion therapy, HT has eventually reached the critical time of transitioning from a limited number of specialized institutions to many particle therapy centres worldwide. Currently, proton therapy is flourishing with around 90 facilities in the clinical practice [3]. About the same number is under construction or planning with around 30 spread across Europe, over 35 in the US. These centres are treating selected tumour patients where radiation damage with X-rays to the surrounding normal tissue could be harmful or even life threatening, such as tumours at the base of the skull, tumours in young children or pregnant women. By the end of 2019 about 250'000 patients have been treated worldwide with Hadron Therapy: more than 213'000 have been treated with protons, about 32'000 with C-ions [3].

Carbon ion therapy is similarly precise as proton therapy but even more effective, since the carbon ions are heavier, and thus deliver more cancer-killing power than protons do. Globally, carbon ion therapy is viewed as one of the next horizons in combatting cancer. In addition to the physical effects of charged particles that allow for a higher conformity, they also exhibit biological advantages that could help to provide better tumour control. While protons have very similar biological effects as photons, heavier particles like carbon and helium ions are more effective in inducing less repairable DNA damage. Moreover, due to their physical properties, they are less dependent on the availability of oxygen in the tumour tissue, and therefore are more effective in the treatment of hypoxic tumours. Treatment with particles with a high Linear Energy Transfer (LET) such as carbon ions is more effective in inducing cell

death than X-ray and protons. For this reason, carbon ions are currently considered the most advanced radiation tool for the treatment of radio-resistant tumours.

Following the pioneering work at Berkeley, in the '50-'90, where carbon and other ions were originally tested, in 1994 the first patient was treated with a carbon ion beam at the dedicated centre at the National Institute of Radiological Sciences (NIRS, Chiba, Japan) [4], which, since then, has been the pioneer centre for this type of radiotherapy. The first in Europe was the GSI "Pilot Project" that treated 440 patients with carbon ions resulting in the construction of the HIT facility in Heidelberg, Germany [5]. The excellent results on several types of cancers obtained in Japan and Germany have encouraged the interest of the oncological community. Since then, around 28,000 patients have received the treatment at 13 centres in Germany, Austria, Italy, Japan, and China. More facilities are under development in South Korea, Taiwan, and France. **Figure 2** shows the current status of HT facilities in Europe/

In order to exploit HT fully for patient specific treatment, there is an urgent need to make extensive range of studies with ion species other than protons and C-ions such as with He, Ne, Be, Li, O, N-ions. This is required to fully understand the Relative Biological Effectiveness (RBE) and to determine the optimal HT ion species for treatment, via *in-vitro* and *in-vivo* studies for a variety of these ions.

Furthermore, new opportunities for improved treatment outcome have recently emerged in connection with new biological mechanisms for potentiating the radiation effectiveness decreasing the normal tissue damage (e.g. combination treatment with nanoparticles, chemotherapy, gene-therapy, immunotherapy or other drugs as well as via ultra-fast "FLASH" irradiation), or expanding the portfolio of usable radiation qualities beyond protons and carbon ions. The exciting recent findings on experiments with very high-dose radiotherapy (>40 Gy/s) in animal models have shown that at high-dose rate normal tissue toxicity is significantly reduced, while tumour control is not affected. The potential advantages in terms of widening the therapeutic windows are enormous and therefore it is important that FLASH radiotherapy studies are carried out both for pre-clinical and clinical research.

In conclusion, the HT field urgently needs research with carbon and other ions, since, despite the recent progress, numerous challenges and new opportunities are yet to be addressed to maximize clinical outcomes and cost-effectiveness of this advanced therapy modality. The goals are: (a) to make it applicable for treating larger number of tumours, (b) to increase accessibility for a greater number of patients globally and (c) to perform cancer research in HT by using multi-ion sources beyond presently used protons and carbon ions, identifying the optimal ion species for HT for each patient [6].

Figure 2: Particle therapy centres in Europe. Courtesy of ENLIGHT, 2020.

1.2 The South East European International Institute for Sustainable Technologies

The South East European International Institute for Sustainable Technologies (SEEIIST) was recently established with the goal of promoting the construction of a new centre for Cancer Therapy and Biomedical Research with Protons and Heavy Ions, based in South East Europe. SEEIIST will enable scientists from different countries to work together in the fight against cancer, promoting scientific excellence and science for peace and development. Moreover, in South East Europe no technical provision exists anywhere to treat patients with certain malignant types of tumours, in contrast to Western Europe.

The present study will analyse and compare different accelerator options, to finally recommend an accelerator development and construction strategy for the needs of SEEIIST. The goal of this new project is to complete the facility design in three years, in order to start accelerator construction at the beginning of 2024. Commissioning is expected to be completed at end of 2029.

1.3 Next-generation carbon therapy accelerators

The main limitation to the availability of heavy ion therapy is the cost of the accelerator. The 2018 Conceptual Study for a new ion therapy and research facility in South East Europe [7] indicates that the accelerator systems count for more than 75% of the construction and operation costs of the facility, in a simple configuration with two treatment rooms and no gantry. When a rotating gantry is included, the accelerator and delivery systems can represent more than 80% of the cost of the facility.

The main goal in the development of ion therapy technology is to reduce as much as possible the cost of the machines, by proposing smaller and more efficient solutions, easing the access to this treatment. Proton therapy has already moved in this direction, bringing the accelerator technology to industrialization and offering compact turnkey solutions that reduce the cost gap with respect to X-ray radiotherapy. The development of carbon ion machines, on the contrary, is still mostly carried out in the framework of research laboratories. Only two vendors, both from Japan, are presently active: Toshiba offering a carbon-ion synchrotron and Hitachi developing the technology.

In comparison, Europe that has played an important role in the development of ion therapy systems is much less advanced. Four facilities are presently in operation in Europe providing both proton and carbon beams for therapy, together with experimental beams of other ions. Two facilities are based on a design jointly developed by GSI (Germany) and Siemens in the period 1998-2008, which resulted in the first facility in Europe dedicated to particle therapy, the Heidelberg Ion Therapy (HIT) centre that treated its first patient in 2009 [5]. A second facility based on a similar design [8], the Marburg Ion-Beam Therapy Centre (MIT) [9], was built by Siemens AG, which, after having also built a second facility in Shanghai, decided to get out of the particle therapy market. The other two European facilities are based on the so-called PIMMS (Proton-Ion Medical Machine Study) design that was developed at CERN between 1996 and 2000 [10]. The first facility built following this model was the Centro Nazionale per Adroterapia Oncologica (CNAO) in Pavia (Italy) [11], which treated its first patient in 2011. The second PIMMS-type facility was MedAustron in Wiener Neustadt (Austria), which treated its first patients with protons in 2016 and with carbon ions in 2019 [12].

Both European designs share similar characteristics, although developed with a different philosophy (compact and industry-driven the GSI/HIT synchrotron as opposed to the flexible and research-oriented PIMMS machine). Because of the normal-conducting magnet technology, their circumference is about 70 m and the acceleration cycle is of the order of 2 s (excluding treatment time). Moreover, they use the same type of linac and source and their carbon beam intensity is limited to less than 10^9 ions per cycle.

Since the design of the European ion therapy facilities, particle accelerator physics has made a remarkable progress, pushed by the requirements of fundamental and applied research. The most visible achievement is the development of reliable high-field superconducting magnets, remarkably validated by the magnet system of the Large Hadron Collider at CERN, whose more than 1’200 magnets operating reliably at unpreceded field strength of 8 Tesla have made possible the discovery of the Higgs particle in 2012. Other developments include: the understanding and control of high accelerating gradients, the higher operating frequencies to reduce dimensions and increase efficiency of linac accelerating systems, the better

understanding and management of multi-particle beam dynamics thanks to more sophisticated computer codes, the development of new layout schemes and finally the widespread use of industrialized components like solid-state high-frequency power systems. The overall trend underlying all these developments has been an effort to reduce size and cost of the facilities improving at the same time their efficiency, to allow a new generation of compact and sustainable accelerators for science, but as well to reach society through the numerous applications of accelerators in medicine, industry, environment, inspection, security, etc [13].

The idea of applying the most recent accelerator technologies to the needs of particle therapy was the main motivation for the Workshop "Ideas and technologies for a next generation facility for medical research and therapy with ions" that took place in June 2018 at the European Scientific Institute of Archamps (France) [14]. The workshop gathered key European and international representatives of both the therapy and the accelerator community to identify the guidelines and to define the specifications for a new generation of particle therapy accelerators aiming at improving the accessibility of ion therapy. Proton therapy being now industrial with four competing vendors on the market, it was felt that the priority of the scientific community was to concentrate on ion therapy. The participants of the workshop agreed that what limits the expansion of ion therapy is the high cost of the accelerator and the limited delivery accuracy due to range uncertainties and duration of treatment. To overcome these limitations, the demands expressed by the medical community were:

- the availability of accelerators with lower construction and operation costs, and reduced footprint;
- a faster dose delivery to patients, thanks to higher beam intensities from the accelerator;
- the use of multiple ions, for more targeted therapies and for range calibration;
- the availability of a gantry system for precise positioning of the beam on the patient;
- the promotion of facilities devoting more time to experiments and testing compared to patient treatment.

Translated into requirements for the accelerator, these *desiderata* mean that innovative accelerator designs are definitely needed aiming at reduced footprint and cost, providing a higher beam flux (particles per unit time), equipped with different ion sources and ready to accelerate diverse ion species, and finally integrating a - preferably small and low-cost - ion gantry. The energy required for carbon ions to treat deep-seated tumours is 430 MeV/u.

A number of accelerator designs have been proposed over the past decade to satisfy at least partially this complex set of requirements, but none has reached the level of being close to implementation. The main options being considered are:

1. A conventional synchrotron with warm magnets, similar to the 2018 SEEIIST proposal [7], equipped in addition with advanced injection and extraction schemes to allow an increase in beam current of a factor 20 and a more flexible operation. This option is discussed in detail in Section 2.
2. A superconducting synchrotron that, on top of the features of the conventional synchrotron, would be a factor 2-3 smaller in circumference (4 to 9 times in surface). A preliminary design [15] is presented in Section 3.
3. A high-frequency linear accelerator (linac) covering the entire energy range, operating in pulsed mode at high repetition frequency [16]. This option, which can be considered as an extension to heavier ions of the on-going development of proton therapy linacs [17] is discussed in Section 4.
4. A rapid-cycling synchrotron, such as the one developed by a collaboration between Brookhaven National Laboratory (BNL) and BEST company [18], which would allow short treatment times thanks to the high pulse repetition frequency.
5. A Fixed-Field Alternating gradient (FFA) accelerator. The PAMELA (Particle Accelerator for Medical Applications) conceptual design of a novel non-scaling FFA for particle therapy was presented in 2013 by a large collaboration based in the UK [19]
6. A superconducting cyclotron delivering a continuous beam. A development in this sense started in 2006 within a collaboration between Ion Beam Applications (Belgium) and the Joint Institute of Nuclear Research (Dubna, Russia) [20] [21]. After a long interruption, it has been recently announced [22] that IBA was restarting this project, aiming at installing a first ion cyclotron in Caen (France).
7. Advanced schemes based on laser production of ion beams and subsequent acceleration, in a laser-based or conventional system [23].

The different alternatives are analysed and compared here, starting from the last one from the list above.

Laser production of ion beams for therapy is only at an initial development stage [23]. Even if the high concentrations of energy, allowed by modern lasers, can extract large quantities of ionized atoms from a target, the techniques required to convert this ion blast into monochromatic beams of controlled intensity and size for therapy are only at a very early stage. Progress will be certainly possible on the long term, but it is unlikely to achieve significant advances within the time available for the design of the SEEIIST facility.

A superconducting cyclotron for carbon ion therapy [21] represents a limit case for cyclotron technology. Although much smaller than that of a warm-magnet synchrotron, the diameter of the superconducting cyclotron (7 m in the JINR-IBA design, which reaches a maximum C-ions energy of only 400 MeV/u instead of 430 MeV/u) is about the same as for a superconducting synchrotron. The total high-field volume in the cyclotron magnet, though, is much larger than the sum of the high-field volumes in the synchrotron magnets, with a correspondingly higher expected cost for the superconducting system. In the case of the cyclotron, injection and extraction are particularly complex; the injection because of the need of multiple ion sources, and the extraction because it must cope with a high amount of beam loss on an extraction septum, the clean charge-exchange extraction being not possible for Carbon ions. Moreover, since the extraction energy from the cyclotron is fixed, additional high-energy beam loss has to be expected at the energy degraders, making activation one of the big limitations in an ion therapy cyclotron facility. We have concluded that the improved treatment flexibility provided by the cyclotron thanks to its continuous beam is not expected to offset its estimated higher costs and its operational limitations because of high activation.

The FFA developed by the PAMELA collaboration for carbon ions is based on two concentric rings of circumference 40 m and 58 m [19]. Even if the footprint is slightly smaller than for a standard synchrotron, the overall accelerator length of 98 m is considerably larger and covered by sophisticated magnets of new design and high cost [24]. Although the non-scaling FFA has some advantages related to its high repetition rate of about 1 kHz and to its variable-energy beam extraction, its high construction and development cost and the large risks connected to its development do not suggest the adoption of this design for the SEEIIST project. New hybrid FFA concepts are presently under study to overcome the limitations of the PAMELA design, but it is too early to take them into consideration for the SEEIIST baseline design.

A rapid-cycling synchrotron, such as the one proposed by [18], pulsing at 15-30 Hz allows an important reduction in the number of ions per pulse with respect to a conventional synchrotron pulsing at < 1 Hz. Although the fast cycling has beneficial effects as faster energy change, simpler injection and extraction, and better control of the delivered dose, these advantages do not justify the substantially higher construction cost and R&D of the fast magnets with respect to a conventional synchrotron. Moreover, it has to be considered that a linac as described in Section 4 can reach a higher pulse frequency than a rapid-cycling synchrotron with lower cost and smaller footprint.

The other three alternatives (linac, advanced warm synchrotron and superconducting-magnets synchrotron) are more promising and will be analysed in detail in this paper in view of selecting the best option for the SEEIIST facility, in terms of: reliability, complexity, time required for development, risk and cost.

2. The advanced warm synchrotron option

In the development line of synchrotrons equipped with conventional warm magnets, the design developed with the support of CNAO for the initial proposal of the SEEIIST facility [7] can be considered as the most up-to-date version of the PIMMS design [10]. An advanced version of this synchrotron, with higher beam intensity and improved injection and extraction, has been designed and analysed. Even if the layout is based on conventional warm-magnet technology, its design parameters and novel features would give it the lead among the ion therapy facilities in the world, with major innovative developments in the dose delivery to the patient, in particular thanks to the multi-energy extraction and a larger stored intensity. This accelerator design is a useful benchmark to which alternative options can be compared.

2.1 Multi-energy extraction and stored intensity

In synchrotron-based facilities, the beam energy is changed directly in the machine, by programming different energy flat-tops for extraction. Presently, in the European facilities, the beam is accelerated to a different energy flat-top and extracted to the patient at every new cycle. Figure 3 shows a sketch of the accelerator operation: every cycle lasts about 2 s (for the magnets) plus a dose delivery spill between 0.1 s to 10 s. A maximum of 10^9 carbon ions per cycle is enough and European facilities are designed to accumulate and store such intensities.

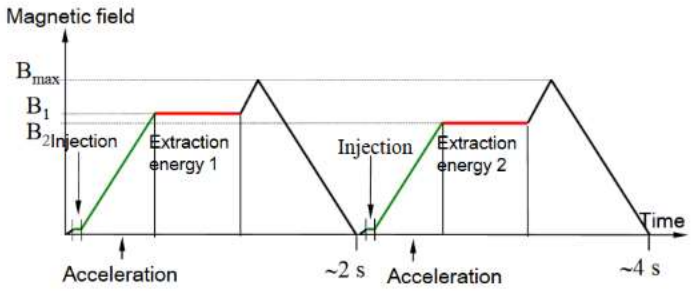

Figure 3: Typical cycle for a synchrotron for medical use with slow extraction. At every new cycle, the beam is accelerated to a different extraction energy, corresponding to a given value of the magnetic field B in the main magnets (Courtesy P. Urschutz, MedAustron).

The NIRS HIMAC centre in Japan [25] developed a new method to maximize the duty cycle and, in particular, to avoid the 2 s waiting time between one energy flat-top and the next. They programmed an operation cycle such as the one shown in Figure 4, with decreasing steps, and managed to successfully extract the beam at different energies within the same cycle.

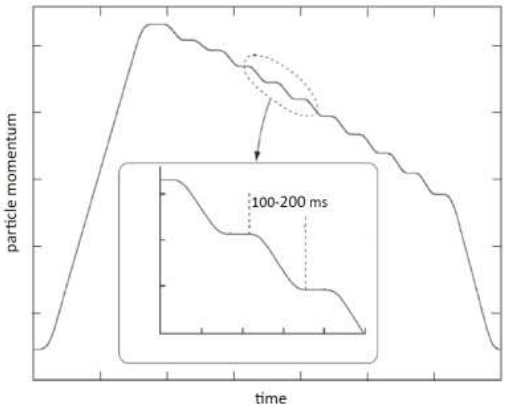

Figure 4: Multiple-energy operation cycle at the NIRS HIMAC particle therapy centre in Japan [25].

To treat a one-litre tumour in one single cycle, the synchrotron needs to store up to 2 10^{10} [26] and this is what the HIMAC team managed to achieve after extensive machine development studies, and having the advantage of a 150 m-long accelerator ring.

The goal for the advanced SEEIIST synchrotron is to be able of storing such intensity by design, which is more than a factor 20 higher than today's European facilities, in a circumference of about 70 m, and perform multi-energy slow-extraction dose delivery.

This choice implies a redesign of the source and injector linac and further development for an advanced multi-turn injection scheme, which will be discussed in the following.

Another novelty of the SEEIIST synchrotron design is that alternative beam pulse structures shall also be available, in addition to the resonant slow-extraction, providing a "standard" beam spill lasting from 0.1

s to 10 s of a maximum 10^9 ions per energy level. In particular, the accelerator will be equipped with a fast (single-turn) extraction system, delivering 2 10^{10} ions in about 1 μs. R&D should be done to assess the feasibility of having a "fast" slow extraction, i.e. delivering the full intensity of 2 10^{10} in less than a second. This will make it possible to apply new treatment modalities, such as FLASH therapy, and extend the experimental programme.

The main parameters for the different ion species to be accelerated in the advanced warm-magnet synchrotron proposed for SEEIIST are summarized in Table 1.

Table 1: Main specifications and beam characteristics of the advanced warm-magnet synchrotron.

Injection/Acceleration	Unit					
Particle after stripping		p	$^4He^{2+}$	$^{12}C^{6+}$	$^{16}O^{8+}$	$^{36}Ar^{16+}$ (*)
Energy	MeV/u	7				
Magnetic rigidity at injection	Tm	0.456	0.91	0.91	0.91	1.03
Extraction energy range (**)	MeV/u	60 – 250 (1000)	60 – 250 (430)	100 - 430	100 - 430	200 – 350
Magnetic rigidity at highest energy (for therapy)	Tm	2.42	4.85	6.62	6.62	6.62
Maximum nominal field	T	1.5				
Max. # of particles per cycle		$2.6 \cdot 10^{11}$	$8.2 \cdot 10^{10}$	$2 \cdot 10^{10}$	$1.4 \cdot 10^{10}$	$5 \cdot 10^9$
Ramp rate	Tm/s	<10				
Ramp-down time of magnets	s	<1				
Spill ripple, intensity ratio I_{max}/I_{mean} (average on 1 ms)		< 1.5				
Slow extraction spill duration with multi-energy operation	s	0.1 – 60				
Fast extraction	s	$\sim 10^{-6}$				

(*) $^{36}Ar^{16+}$ is for research only, not for treatment

(**) Energy range within which the beams are compliant with clinical specification. In parenthesis, the higher energies possible for p radiography and imaging and He radiography.

Table 1 reports the intensities needed for the ions in therapy. Those are scaled in order to have the same dose deposited in the reference one-litre water-equivalent tumour, according to the following formula [27] that expresses the range of hadrons in water R^{water} as:

$$R^{water} = (425 \text{ cm}) (A/z^2) (K / Mc^2)^{1.82}$$

The mass number A enters because Mc^2 has been expressed as A×931 MeV. K is the ion kinetic energy and z is its atomic number. With proper setups, all species between p and Ar can be accelerated. Lithium might also be used for therapy, with intensity of 4.7 10^{10} ions/pulse. Argon is used only for research purposes. The baseline layout foresees three ion sources permanently installed in front of the accelerator, one for protons, a second one for Carbon, and the third one to be used for all other ion species.

Figure 5 shows the optimized layout of the accelerator system, including the transport lines to three treatment rooms (one equipped with gantry) and two experimental rooms as specified for the SEEIIST facility.

The accelerator is the 25 m diameter PIMMS synchrotron of [7], with the additional features described here. The ions are produced in one of the three sources and pre-accelerated to 7-10 MeV/u in a linac before being injected in the main synchrotron. Contrary to the PIMMS accelerator, here the injection and extraction are performed in the two opposite straight sections.

After the energy for treatment is reached (for carbon ions it is in the range from 100 MeV/u to 430 MeV/u, see Table 1, depending on the depth of the tumour), the beam is extracted to the high-energy transfer lines and sent to the treatment and experimental rooms.

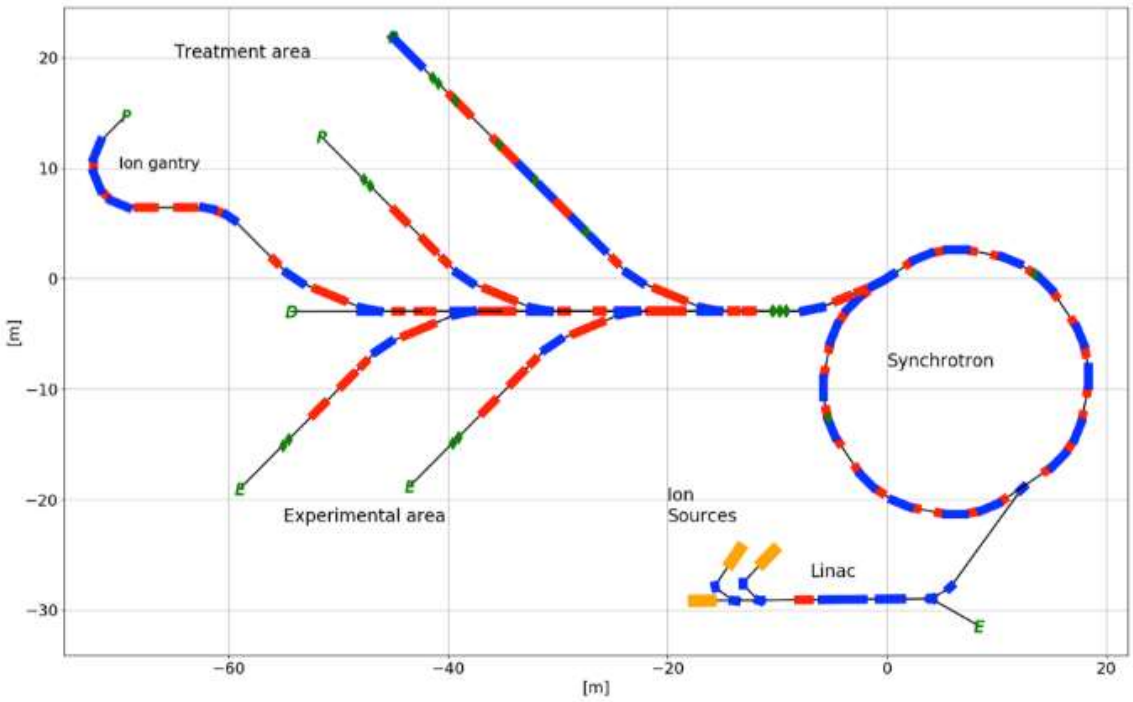

Figure 5: A preliminary layout of the accelerating and beam delivery components of the SEEIIST facility. The upper beamlines are dedicated to patient treatment while the lower ones provide beam for radiobiology and materials research.

2.2 Layout

The synchrotron is based on two symmetric, achromatic arcs joined by two dispersion-free sections [7] [10], as shown in **Figure 6**.

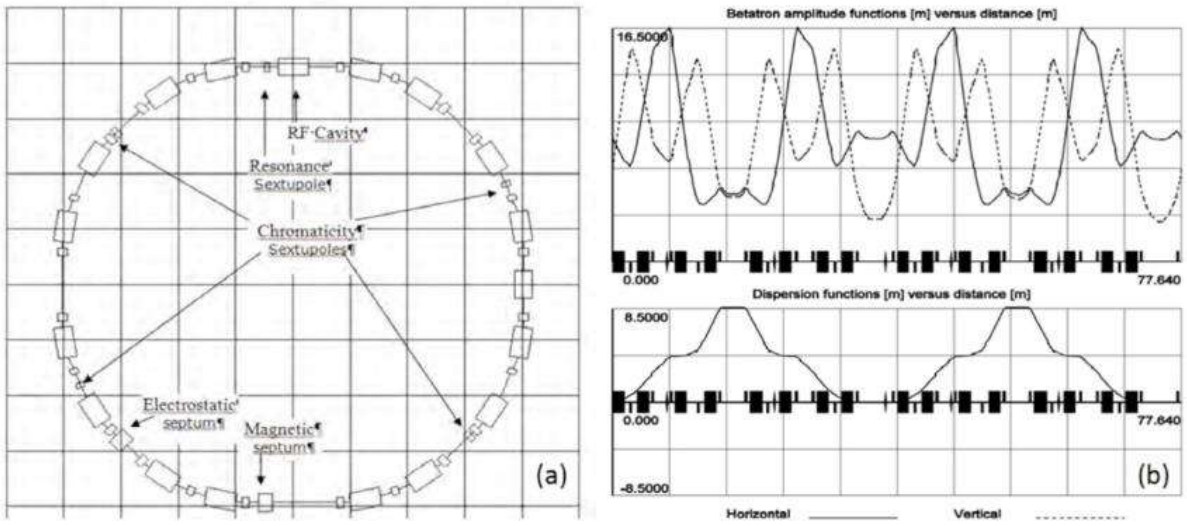

Figure 6: (left) Layout of the baseline synchrotron with warm magnets. (right) Optical functions: betatron functions (above) and dispersion (below) [10].

The synchrotron has 16 dipoles. The 24 quadrupoles are grouped in three families that allow enough flexibility to match all the needed tunes while conserving the dispersion free regions. The 4 chromaticity sextupoles are grouped in 2 logical families and are placed such that it is possible to change independently the horizontal and vertical chromaticity; these magnets are individually powered to allow some additional flexibility in setting up the extraction.

For the orbit correction, there are 8 vertical beam position monitors with the same number of associated vertical correctors and 10 horizontal monitors with their associated correctors.

In one of the two dispersion-free sections, there is the magnetic extraction septum. In the other one there are the resonance-driving sextupole and the injection electrostatic septum. The injection and extraction orbit bumps are created with 2 horizontal kickers for each one, positioned at a proper phase advance.

The RF system will consist of a 0.47-3.26 MHz Finemet® loaded wideband cavity. This cavity will be powered by solid state amplifiers connected to a digital Low-Level RF (LLRF) system, as done for MedAustron [28]. These are state of the art cavities for low-energy accelerators [29] and easily allow operation in multi-harmonics mode. This technology has been successfully tested and now is being deployed for the upgrade of the CERN PS Booster [30], to increase the bunch length and reduce space-charge. Contrary to PIMMS design, the RF-cavity is located in a non-zero dispersion section, which is a choice common to other accelerators, such as the CERN PS Booster, and in general rings where dispersion-free sections are not available.

The beam from the linac is multi-turn injected into the synchrotron to reach the required intensity as described above.

Extraction is performed by RF-Knock Out (RF-KO) at multiple energies during the same accelerator cycle. Moreover, the ring is equipped with a fast extraction system as well, to extract the entire beam intensity in a very short pulse, of the order of 1 μs, for research and eventually treatment of the FLASH dose delivery modality. The extraction process is presented in detail in [31].

2.3 Injection

The main challenge for SEEIIST is the increase of the beam intensity up to 2 10^{10} ions/pulse. This is possible by the increase of the ion source intensity, a better transmission through the linac and the optimization of the multi-turn injection process.

Figure 7 shows the results of the simulations of the multi-turn injection process [32], to achieve 2 10^{10} carbon ions accumulated in the accelerator.

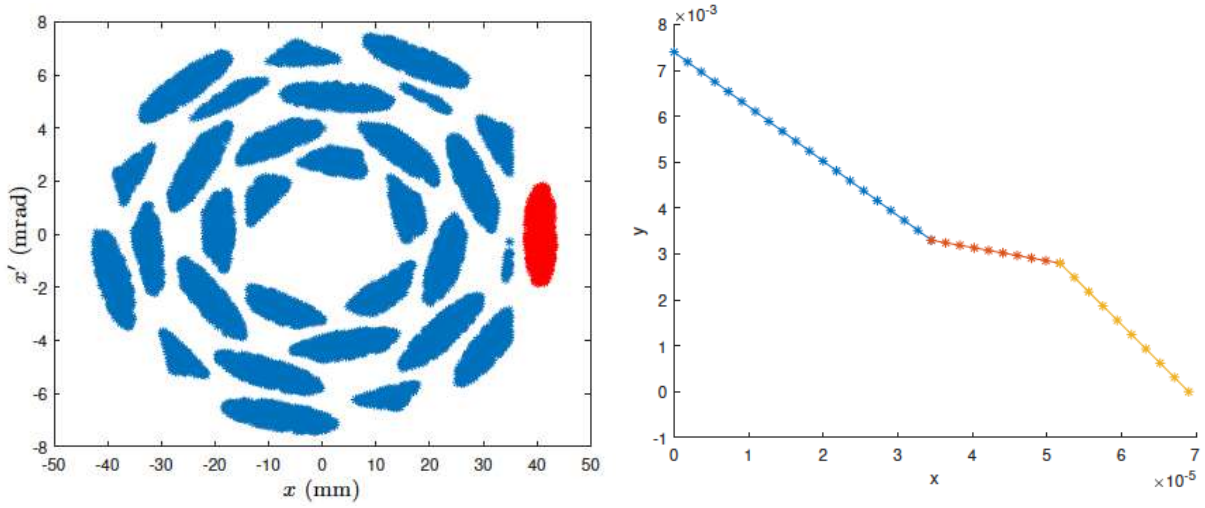

Figure 7: (left) Phase space of the circulating beam after 30 turns in blue. The injected beam from the linac is in red. (right) Kicker strength (rad) as a function of time (s), to produce an orbit bump of 44.7 mm at the injection septum location.

The function of the kicker strength, which provides an orbit bump varying with time, has been optimized to maximize the intensity and minimize the emittance of the circulating beam after a 30-turn injection. Increasing further the number of injected turns dilutes the emittance excessively. Table 2 summarizes the optimal set of injection parameters and the resulting beam characteristics.

Table 2: Optimized parameters for injected and circulating beam.

Number of injected turns	30
Injected beam emittance	0.7 μm
Horizontal tune	1.82
Ratio of β function of injected beam and the circulating beam	0.5
Effective numbers of injected turns (injection efficiency %)	21 (70%)
Resulting circulating emittance	5.6 μm

The effective number of injected turns N_{eff}, defined as the injection efficiency multiplied by the number of turns (i.e. 30), is 21. Using the formula below, it results that the current needed from the source at the injection point (including the linac transmission efficiency) is 354 μA, within a 0.7 μm normalized emittance. These values are considered feasible with the new generation Electron Cyclotron Resonance (ECR) sources, as discussed later in the section:

$$I = \frac{qeN_{eff}}{t_{rev}}$$

where q=4 is the charge state of the C-ions from the source, before the stripping foil, e is the electron charge and t_{rev} is the revolution time, i.e. the time needed to complete one turn in the synchrotron.

The final circulating horizontal rms normalized emittance is 5.6 μm, which is much larger than the 1 μm expected in the standard PIMMS-type synchrotron for a 10^9 C-ion beam. Similar optimized simulations showed that, in order to inject 2 10^{10} Carbon ions and keep the emittance below 1 μm, N_{eff} is only 7.8. This would require a current from the source of about 1 mA (including the linac transmission), which is presently not feasible. Alternatives to reach such intensities in a small emittance would be to have a different type of source, called Electron-Beam Ion Source (EBIS), characterized by a much smaller emittance but which still requires significant R&D, or to conduct a more complicated multi-turn injection process.

The stored beam will therefore be flat, with a normalized horizontal emittance of 5.6 μm and a vertical emittance of 1 μm. Such a value for the vertical emittance is required for the gantry operation and is similar to the value of the PIMMS design. Careful studies and machine-development experiments need to be conducted to prove that such a flat beam can be stored and accelerated without emittance exchange. This can be done by properly compensating resonances to avoid losses, as is done e.g. in the CERN PS Booster for the ISOLDE beams. Moreover, the slow-extraction shall be revised taking into account the new horizontal beam dimensions.

2.4 Injector linac layout and alternatives

The standard injector linac, as the HIT injector shown in **Figure 8**, is composed of ion sources, low-energy beam transport lines, Radio-Frequency Quadrupole (RFQ) accelerator, accelerating structure and stripping foil. All the European facilities share a similar design [33], originally developed between GSI and Frankfurt University in the early 2000s. The ion sources are followed by a 1-metre long 4-rod RFQ and by a 4-metre long Interdigital H-mode Drift Tube Linac (IH-DTL) accelerating structure. Both structures operate at 216 MHz and are designed to accelerate C^{4+} ions (q/m=1/3) to 7 MeV/u, after which the remaining electrons are stripped and the beam is injected to the synchrotron. The Japanese facilities use injectors at a similar frequency of 200 MHz; however, their final energy is only 4 MeV/u.

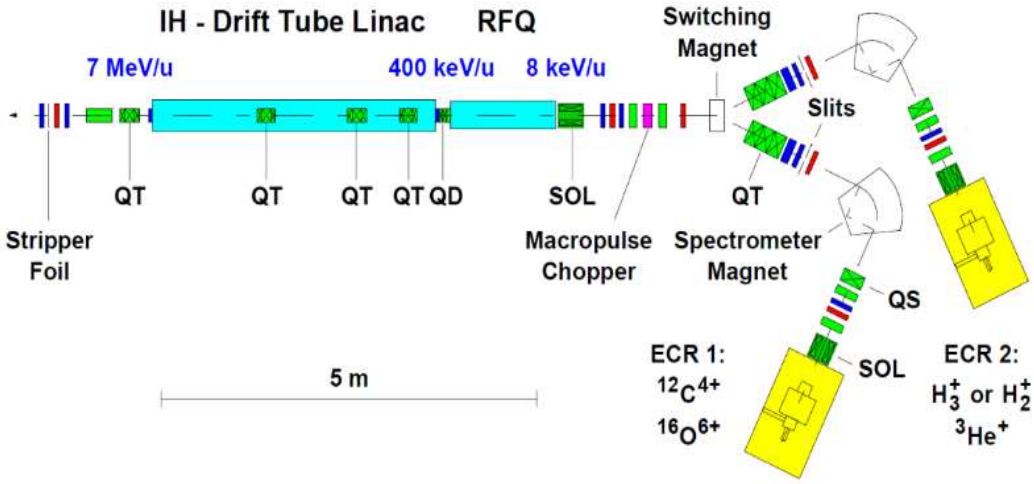

Figure 8: European "standard" injector-linac design based on developments of GSI and Frankfurt University in the early 2000s [33].

The European standard linac has low repetition rate and duty factor (5-10 Hz with duty factors only 0.1-0.3%) and requires a peak Radio-Frequency (RF) power of about 1 MW provided by tube-based RF amplifiers. The overall beam transmission, between ion source and stripping foil, is about 50%. This design, although compact and robust, is about 20 years old and new linac technologies could be used to reduce the cost and improve availability of the injector linac.

In the original reference SEEIIST design [7], the linac accounts for about 25% of the total cost of the accelerator. Indeed, its further cost optimization is one of the main objectives of a new design. The other objective is the increase of current within the beam pulse, which can be done by increasing the overall transmission, and by increasing the ion source current and/or decreasing its emittance. The final energy should not change, as 7 MeV/u is already optimal, although a higher energy of 10 MeV/u is reachable and might help to accumulate a larger beam intensity in the synchrotron.

Recent years have seen a clear trend towards increasing the operating frequency of low-energy injector linacs. This allows for higher acceleration efficiency and for smaller dimensions of the accelerating structures, both parameters with a strong impact on the overall cost. Although the trend is particularly visible for proton linacs (Linac4 at CERN and the p-Linac at GSI operate at 352 and 325 MHz,

respectively), designs have been made for ion linacs operating, in the low-energy part, at frequencies as high as 750 MHz (as the linac described in Section 4 of this paper).

Superconducting technology can be used as well for low-energy linacs. However, the need to have short focusing periods for control of beam emittance imposes the usage of short cavities spaced by warm quadrupoles. This results in a low "real-estate" accelerating gradient (i.e. averaged over the entire accelerator length) that becomes comparable with that of warm structures. Additionally, the reduction in RF power, which is the main advantage of superconducting cavities, cannot be fully exploited in the case of a synchrotron injector operating in pulsed mode at very low duty cycle. Therefore, superconducting technology was not considered for an upgraded injector linac for this project.

Because of the stringent requirements in terms of accelerated current in the synchrotron, the ion sources for the SEEIIST linac have to provide about four times higher beam currents than the standard ECR Ion Source SUPERNANOGAN [34] used in the existing facilities, which delivers an average of 260 μA of C^{4+} ions in a normalized emittance of about 0.7 μm. The new SEEIIST specifications can be met by ECR sources of a new design; for example, the new PK-ISIS source [35] being commercialised by the company Pantechnik, or the new AISHA source [36] being developed in the INFN LNS laboratory at Catania. However, those sources are significantly larger and power-demanding than SUPERNANOGAN, which is based on permanent magnets; therefore, a significant space and additional power must be foreseen. The SEEIIST facility will have at least three ion sources, two producing ions for therapy and research (in particular helium, carbon, oxygen) and a third one producing only protons.

The installation of a fourth source, an EBIS, based on a different operation principle [37] is being considered. EBIS produce beams with significantly smaller emittance (i.e. smaller than 0.1 μm) and would allow a more efficient multi-turn injection into the synchrotron, with the result of producing beam with intensities and brightness up to the space-charge limit of the accelerator. Currently, the EBIS still require a significant R&D to be competitive with the ECR source in terms of intensity and reliability. On the other hand, the ECR sources can efficiently generate only partially stripped ions, like C^{4+}. This charge state of Carbon is also very good for beam purity, as there are no common isotopes which have the same charge-to-mass ratio while the C^{6+} produced by the EBIS can be contaminated by alpha particles or other ions with the same charge-to-mass ratio ½.

The low-energy beam transport (LEBT) is a set of beamlines between the sources and the RFQ. The role of LEBT is to select the isotope for further acceleration, transport the beam and allow for fast switching between the ion sources. A modern LEBT needs to incorporate analysing dipoles, fast-switching dipoles, solenoids, quadrupole magnets, electrostatic chopper and instrumentation.

For the main part of the linac, comprising the RFQ and accelerating structures, a preliminary analysis leads to two most promising concepts, as summarized in Figure 9.

The first one assumes an increase of the linac frequency to 325 MHz or 352 MHz. At those frequencies, the RFQ can be built using a 4-vane design like at CERN Linac4, or a more economical 4-rod "ladder" design as the RFQ being built by the Frankfurt University for the new GSI proton injector. The accelerating structure can be Alvarez, Quasi-Alvarez or CH-type. One of the possible advantages of the increased frequency is the possibility to use a single klystron, as a power source for the whole linac, followed by a power splitter with the proper ratio of power between the RFQ and the following structure. The high peak power available from a standard 325/352 MHz klystron, about 2.8 MW, would permit an increase in the acceleration gradient and a further reduction in the length and cost of the linear accelerator. Although economic, this solution might be complex to realise from the RF point of view. A suitable alternative would be using solid-state RF amplifiers, which have higher cost, but are very reliable and require less maintenance than a klystron-based RF system.

The second concept assumes the use of the new 750 MHz RFQ design, recently developed at CERN, followed by a 750 MHz Quasi-Alvarez Drift-Tube Linac. The CERN 750 MHz RFQ can provide efficient

acceleration of fully stripped carbon ions up to an energy of about 4-5 MeV/u. The design of this RFQ is described in Section 3 and can be directly adopted for the injector in the case of an EBIS source. For an ECR source, the design has to be redone for C^{4+}.

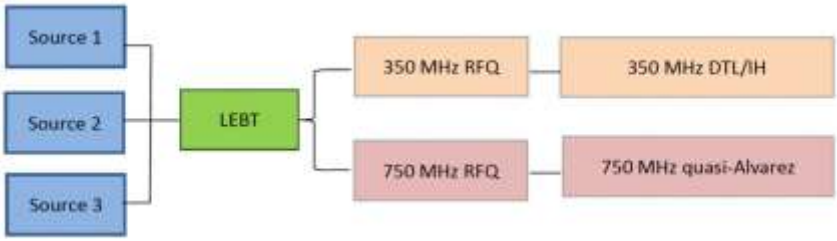

Figure 9: Two alternative concepts for the injector linac.

2.5 Alternative ring layout

The baseline for the warm-magnet synchrotron option is the improved PIMMS design discussed so far, but in parallel, other layout options, alternative to PIMMS, have been explored and will be considered for further studies. Two directions have been considered: to improve the basic lattice of PIMMS or to go to completely different lattice structures.

All ion therapy synchrotrons share a similar lattice structure, based on FODO cells, i.e. the alternation of Focusing (F) and Defocusing (D) quadrupoles, interleaved by drift (O) spaces, which are normally filled by the dipoles. They are the simplest structure, but they have no dispersion-free sections, which is a desired requirement to simplify injection, acceleration, and extraction dynamics. In order to have two long straight sections with zero dispersion, in the present reference design the FODO lattice of PIMMS has been modified and a third quadrupole family has been introduced to guarantee such a property, making it a FODOF lattice.

The University of Melbourne is developing an alternative lattice [38] based on a Double-Bend Achromat (DBA) cell, in collaboration with the SEEIIST design team that is sharing basic parameters and experience. The choice to start from a DBA is mainly driven by the preference for dispersion-free drift sections. In comparison with a compact PIMMS-type FODOF lattice, the DBA requires a smaller number of quadrupole magnets and independent power supplies.

The DBA was initially designed as a candidate for electron storage rings where small beam divergences and very low emittance in long drift sections are required to accommodate insertion devices.

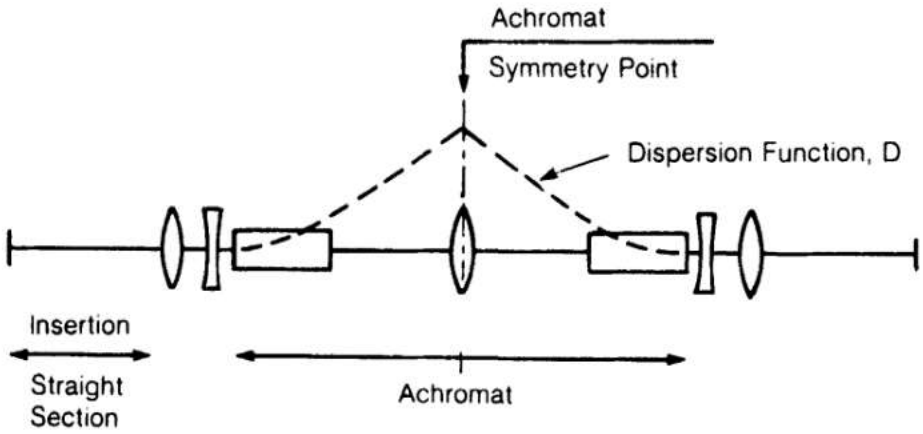

Figure 10: Schematic of a Double Bend Achromat (DBA) cell, which consists of two dipoles and five quadrupoles arranged symmetrically [39].

First, two 180^0 DBA cells were joined together to form a closed ring with two dispersion-free long drifts. The bending length per cell is adjusted to 27.72 m corresponding to a maximum dipole field of 1.5 T. Each

dipole section was subdivided into three dipoles that are each 2.31 m long. An additional quadrupole was added symmetrically on both sides of the central quadrupole to achieve a tune that is close to the third integer. It was necessary to shift the additional quadrupoles along the ring by one dipole element to provide the required phase advance between the elements for the slow-extraction scheme.

The extraction sextupole and the RF-cavity are located at one of the dispersion-free sections, while both injection and extraction magnetic septa are located at the other dispersion-free section. The choice of the septa arrangement potentially limits the orientation of injection and extraction to opposite sides of the ring. It is possible to swap the injection septum with the RF cavity by increasing the length of the dispersion-free drift length. The electrostatic septum is placed at a proper phase advance from the extraction magnetic septum and at a relatively large horizontal beta function. The Hardt condition is satisfied [40]. Space is reserved in dispersive regions along the ring for a pair of chromaticity sextupoles. As such, the chromaticity of the machine and the resonance conditions can be controlled separately. Additional work is required to include bump magnets for injection and extraction. The vertical betatron envelope was optimised by varying the drift lengths and quadrupole strengths.

Figure 11 shows the schematic layout and the lattice functions of the final optimised design and the detailed parameters of this design are presented in Table 3.

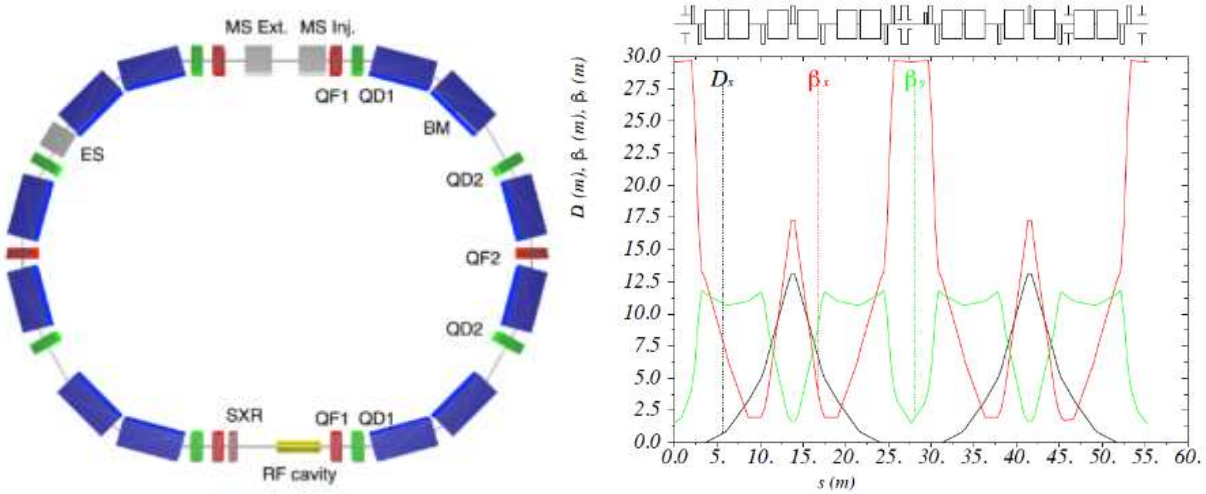

Figure 11: (left) DBA-based synchrotron lattice layout and (right) Twiss functions [38].

Table 3: Detailed parameters of the proposed DBA lattice [38].

Circumference length	55 m
Max energy	430 MeV/u
Dipole length	2.31 m
Max dipole strength	1.5 T
Working point (Q_x,Q_y)	(1.67, 1.72)
Transition gamma γ_t	1.742
Natural chromaticities ξ_x, ξ_y	-1.1,-1.3
QF1 strength	1.05 m^{-2}
QF2 strength	0.8 m^{-2}
QD1 strength	-1.3 m^{-2}
QD2 strength	-0.65 m^{-2}

The synchrotron has in total 12 dipoles and 14 quadrupoles. It is smaller and less complex than the PIMMS design, still keeping two zero-dispersion straight sections.

3. The super-conducting synchrotron option

Taking inspiration from the NIRS developments [41], in 2018 the TERA Foundation developed a compact superconducting synchrotron design, characterized by the fact that the same 90° magnet unit is used for both the synchrotron and the gantry [15]. As an additional novelty, the design is based on Canted-Cosine-Theta magnets with Alternating Gradient (AG-CCT). This design has been refined and developed, to be considered as an alternative for the SEEIIST.

3.1 Magnets technology and ramp-rate

The AG-CCT technology allows to have curved magnets and nest alternating-gradient quadrupoles inside. A design in this sense was developed by LBNL [42], for a single-pass system, i.e. a large acceptance medical gantry. Examples of AG-CCT magnets are shown in **Figure 12**.

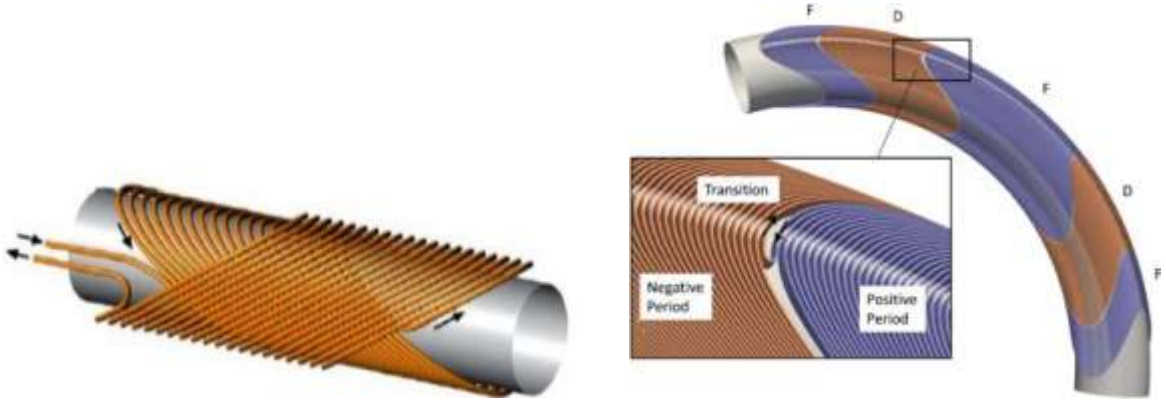

Figure 12: Examples of CCT magnets. (left) Pure dipole: the two vertical magnetic fields produced by the two coils cancel along the tube axis and add in the transverse direction. (right) AG-CCT: Windings needed to obtain sections that are alternatively focusing (F) and defocusing (D) [42].

A CCT magnet consists of a pair of tilted, i.e. canted, coils designed such that their transverse- fields sum and axial fields cancel [43] [44]. The large number of individual turns, approximating the $\cos(n\theta)$ axial current distribution, naturally leads to a high level of field quality without the need for optimization of conductor placement in blocks or sectors typical of other magnet designs. These benefits are offset by the use of more conductor in CCT designs (typically 20-30%) as compared to traditional magnets, which makes the choice justified up to about 4 T. Curved versions of CCT magnets might be easier to build than conventional cosine-theta magnets and the wires would be subject to much smaller mechanical stress. A major advantage is that it is relatively easy to add nested quadrupoles in the form of additional magnet layer, alternatively focusing and defocusing within the bending magnet.

A major R&D on the magnets is needed to achieve a ramp-rate of 1 T/s. The cycle length will be of 6 s minimum, a factor 3 longer than the one for the normal-conducting version. Accumulating a large beam intensity and performing multi-energy extraction is a key requirement to reduce the impact of the magnet ramp-time on the total treatment time.

3.2 Layout and beam optics

Figure 13 shows the proposed layout and footprint of the accelerating and beam delivery structures of a superconducting magnet version of the SEEIIST facility. It is based on a 27 m circumference synchrotron, an injector linac and four particle sources, an extraction beam line and a gantry, of external radius of 5.0 m. Both the synchrotron and the gantry make use of 90-degree AG-CCT superconducting magnets.

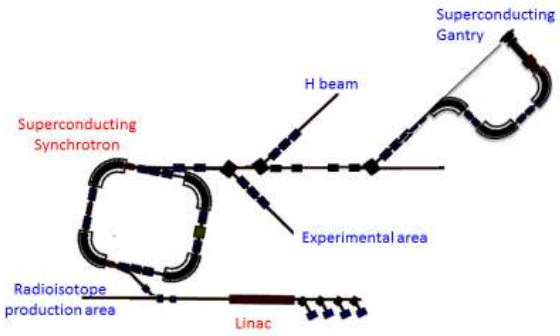

Figure 13: Schematic view of one of the possible layouts of the superconducting facility [15].

The advantages of this design and the large footprint reduction obtained by using superconducting magnets become evident in the comparison with existing facilities based on the PIMMS design, shown in **Figure 14**.

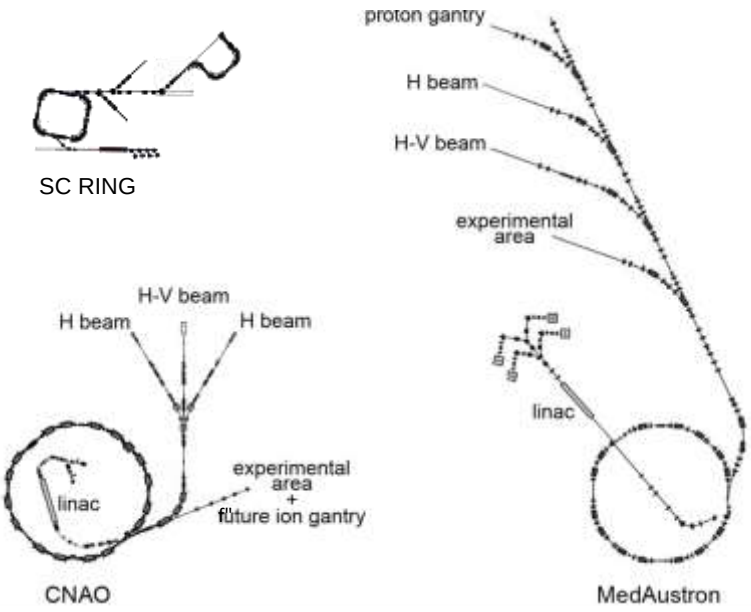

Figure 14: Comparison of the footprints of the proposed SC ion therapy facility with the one of CNAO and MedAustron [15].

The ring consists of four 90^0 CCT magnets and it has a two-fold symmetry where the straight sections for the injection and extraction systems are kept as short as possible, as sketched in Figure 15.

The main 90^0 CCT magnet units were modelled as four combined-function sector-bend magnets of 22.5^0 each, carrying a quadrupole component either focusing or defocusing of the same absolute amplitude. Two short straight sections of 25 mm are also included at the beginning and end of each bending sequence to take into account the space needed for the return coils and the cryogenic vessel.

The four main magnets are powered in series, as well as their nested quadrupoles. To add tunability, two extra families of small, air-cooled quadrupoles are added in the four straight sections.

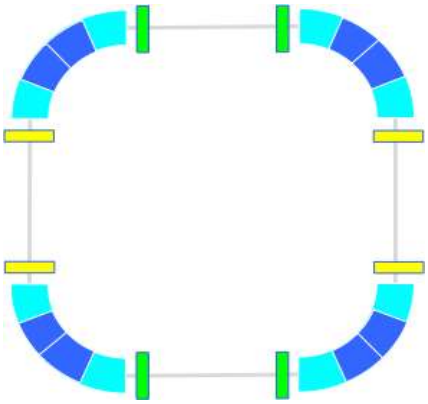

Figure 15: Sketch of the synchrotron ring elements' layout: in blue the main 90^0 magnet units, with nested quadrupolar focusing and defocusing, components. In yellow and green the two families of small air-cooled quadrupoles for tuning [15].

The working point during the slow-extraction process is positioned close to a third order resonance, in this case the $3Q_x = 5$, while during injection and acceleration, it is safely far from the resonance and optimized for an efficient multi-turn injection. The accelerator is working below transition, as it is usual for small rings.

Parametric studies have been carried out to identify the optimum length of the focusing and defocusing component inside the magnets and their gradient *kb*, the length of the two straight sections and the strength of the two air-cooled external quadrupoles families *kq1* and *kq2*. The goal was to:

- minimize the maximum horizontal and vertical beta-functions and dispersion;
- work below transition and reach the desired horizontal tune, keeping away from resonances.

Figure 16 shows an example of parametric study, in which the length of nested quadrupoles and straight sections are fixed and the effect of varying the gradients of the nested quadrupoles ±*kb* and of the external quadrupoles *kq1=kq2=kqq*, are explored. In this example, one can identify a region around *kb* ~ 0.7 m^{-2} and *kqq* close to zero for which the tunes are about $Q_x = 1.68$, $Q_y = 1.1$, gamma transition $\gamma_t > 1.5$ and the maximum vertical beta function $\beta_y < 14$ m. Once a good starting point in terms of parameter region is found with this method, the usual MADX [45] matching routines are employed.

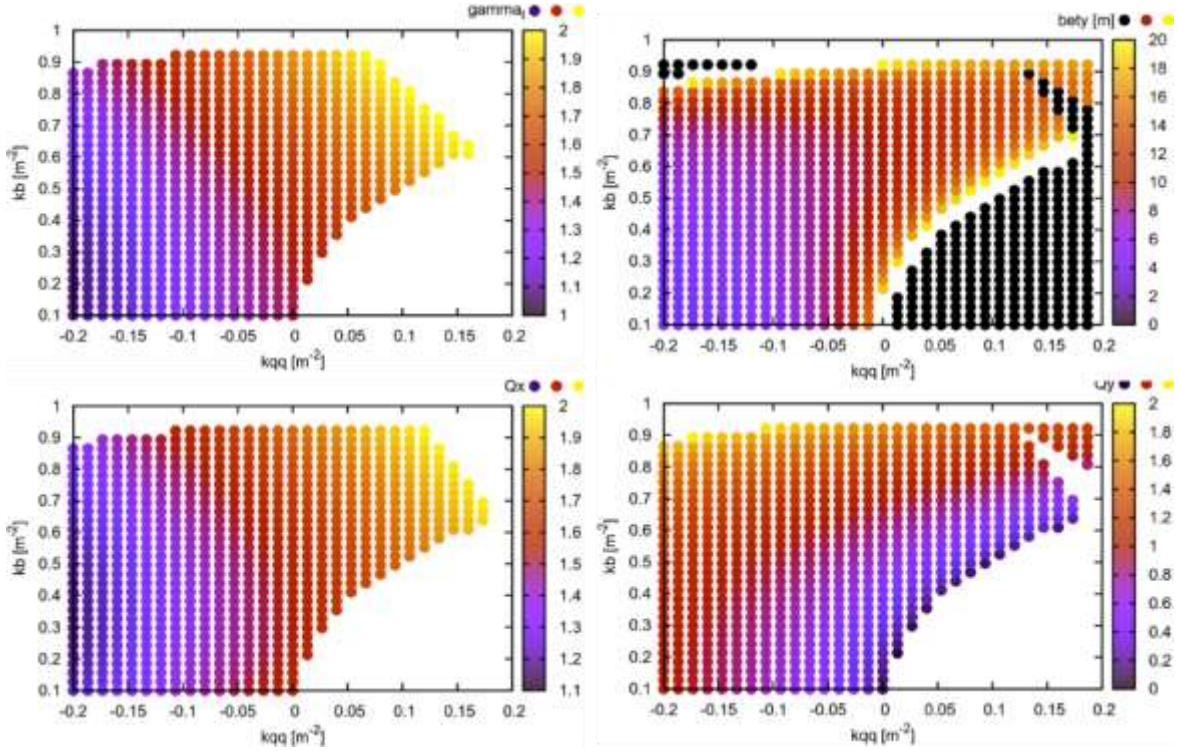

Figure 16: Example of parametric study to find the optimum working point area. The effects on γt (gammat) in the figure), βy (bety in the figure), Qx , Qy of the variation of ±kb (gradient of the nested quadrupoles) and kqq (gradient of the external quadrupoles, assuming the two families have the same strength) are shown [15].

A lattice with a horizontal tune close to $Q_x = 1.68$ was obtained. This working point is close to the third order line $3Q_x = 5$ used for the slow extraction and can be moved far off the resonance for injection and acceleration. **Table 4** summarizes the accelerator dimensions and magnets specifications.

Table 4: Superconducting magnet synchrotron dimensions and parameters [15].

Circumference	C	27 m
Injection energy		10 MeV/u
Extraction energy		100 → 430 MeV/u
Straight section 1	d1	3 m
Straight section 2	d2	3.6 m
AG-CCT Max. bending field	B	3.5 T
AG-CCT Bending radius		1.89 m
AG-CCT Magnetic bending angle		90°
AG-CCT Quadrupole alternation		FDF (22.5°-45°-22.5°)
AG-CCT Straight section length at extremities		25 cm
AG-CCT Max. quadrupole field		10 T/m
AG-CCT Radius of vacuum chamber		70 mm
External quadrupole length	lq	0.1 m
Distance between bend and quad	dq	0.1 m
Max. Gradient of quadrupoles section 1		10 T/m
Max. Gradient of quadrupoles section 2		10 T/m

Figure 17 presents an optics with the horizontal tune at exactly $Q_x = 1.68$, for extraction. A vertical tune $Q_x = 1.13$ has been chosen. In this specific case, the aim was to have, for the extraction process, a dispersion "as small as possible" in the long straight section where the extraction septum is located.

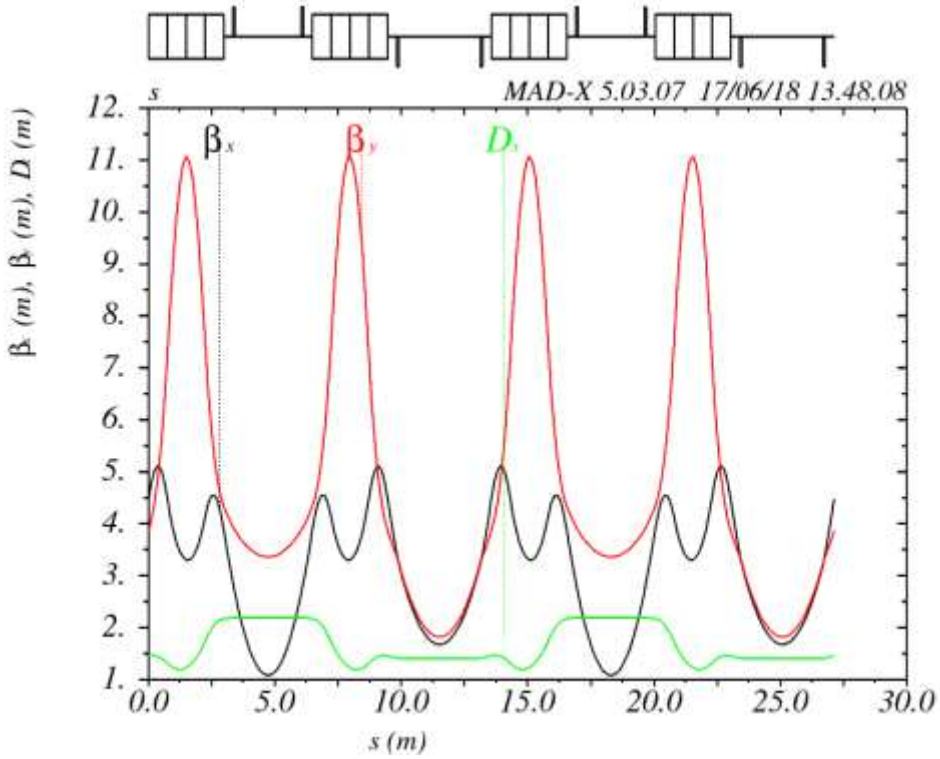

Figure 17: Optics functions at extraction (working point of $Q_x = 1.68$, $Q_y = 1.13$) [15].

Table 5 summarizes the parameters for the extraction optics.

Table 5: Optics parameters, for a working point of $Q_x = 1.68$, $Q_y = 1.13$ [15].

Normalized strength of nested quadrupoles	kb=kbf=-kbd	0.69 m^{-2}
Normalized strength quadrupoles section 1	kq1	0.17 m^{-2}
Normalized strength quadrupoles section 2	kq2	- 0.95 m^{-2}
Gradient of nested quadrupoles @ 430 MeV/n		4.56T/m
Gradient of quadrupoles section 1 @ 430 MeV/n		1.12 T/m
Gradient of quadrupoles section 2@ 430 MeV/n		- 6.27 T/m
Horizontal tune	Q_x	1.68
Vertical tune	Q_y	1.13
Transition Gamma	γ_{tr}	1.683

During injection and acceleration, the horizontal tune is at about $Q_x = 1.72$, thus far from the resonance. The working point is changed by varying the current in the nested quadrupoles of the main magnets and by trimming the other two external quadrupole families. The final γ_t is always higher than 1.5, thus ensuring operation below transition.

3.3 Alternatives to superconducting synchrotron layout

The choice for the superconducting magnet design [15] was to have a Focusing-Defocusing-Focusing (FDF) structure, with the inner defocusing coils extend for twice the length of the focusing components.

Another interesting option would be to alternate a sequence of FDFDF to get closer to the design of a DBA. However, the simulations did not show a dramatic advantage going in this direction. The major constraint for the operating point is to achieve a large enough γ_t in order to work below transition, and this leaves limited possibilities. Moreover, due to the design of the AG-CCT layers [42], i.e. because the coils are winded to achieve both the focusing and defocusing component, there is a given amount of current flowing in the wires and therefore, the integrated strength of the quadrupoles is simply proportional to its length. It would be interesting to have e.g. a strong focusing component in the middle of the dipole and a weak defocusing effect in the extremities, again to approach the DBA design.

For this, other options have to be investigated in future studies, as for example:

- have a nested focusing quadrupole only in the middle;
- have a nested focusing quadrupole in the middle and a defocusing combined-function magnet everywhere;
- move away from the AG-CCT design and split the 90^0 bending unit in three parts, as in the NIST design [46];
- consider different ring super-periodicity and layouts, as an example a triangle with three straight sections.

4. The full linac option

In the past years, the idea of using linear accelerators has been developed, initially for proton therapy, due to the advantages it would bring in terms of costs and therapeutic beam quality [47, 17].

At present, there are worldwide two medical proton linacs being commissioned, while linacs for carbon ions are still at a conceptual stage in a handful of research centres. In this section, the beam-dynamics design of a 3 GHz linear accelerator for carbon-ion therapy, from the pre-injector to the very end of the linac, is described. It is based on the work done at CERN on a proton machine [17] and after the proposal of the TERA Foundation [47] [48]. The end-to-end beam tracking demonstrates the potential capability of the machine of providing extremely high-quality beams at very high repetition rates, specifically tailored for carbon ion treatment.

The main advantage of a full-linac accelerator for ion therapy is that, contrarily to the synchrotron, a linac can be pulsed at high-repetition frequency, 100 Hz or more, keeping a different number of accelerating cavities active for each pulse. This provides a simple, efficient, and rapid way to change the beam energy in order to "paint" longitudinally the tumour, depositing the dose at different depths. The energy modulation has been, so far, demonstrated on an experimental full linac for proton therapy (ADAM-AVO) but the accurate control of the dose to the patient has still to be demonstrated.

The accelerator footprint heavily affects the cost of a carbon-ion therapy facility. A 50 m long linear accelerator is not suitable to fit into an existing hospital facility. The footprint can be improved by reducing the ratio between the longitudinal and the transverse dimensions of the machine, adapting the design from a completely linear to a more rectangular solution. For this reason, a "bent-linac" design, with a curved section of 180^0 in the middle, has been adopted. The purpose is to optimize the footprint to fit in a rectangular room, while preserving the high beam quality that characterizes linear accelerators.

The frequency adopted for acceleration in the main linac section is 3 GHz, as for the proton therapy linacs, while the frequency of the injector section is 750 MHz.

4.1 Layout

A schematic of the bent-linac version [16] and all its components is shown in Figure 18.

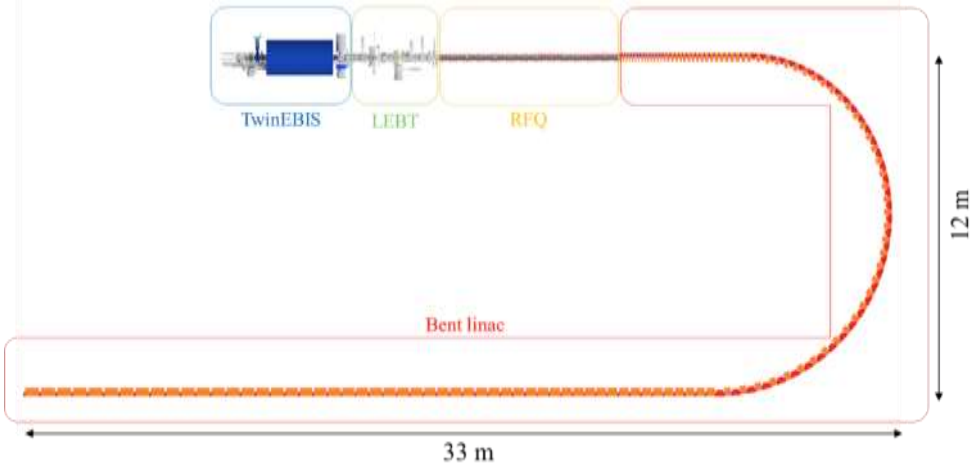

Figure 18: Layout of the bent linac [16]

Because of the high operating frequencies, the full-linac option can accelerate only particles with a minimum charge to mass ratio (q/m) of 0.5. Therefore, it requires a special ion source development to reach the design beam current that cannot be provided by commercial ion sources of the ECR type for such a high q/m.

In the present design, the $^{12}C^{6+}$ ions needed for treatment are generated in a TwinEBIS source which can generate 10^9 ions in a 5 μs pulse at the repetition rate of 200 Hz. Such a source is presently under commissioning at CERN [49]. After the source, the ions are extracted and transported into the Low-Energy Beam Transport (LEBT), where they are accelerated up to 15 KeV/u. The LEBT allows to match the beam parameters to optimize the transmission into the RFQ.

The 750 MHz RFQ is the first RF accelerating structure and boosts the particles' energy up to 5 MeV/u. The design was optimized to minimize the power consumption and the material costs and to prepare the beam for the injection into the 3 GHz linac without losses.

The 3 GHz bent linac, coming downstream the RFQ, can be divided in three sections, each one with its own specificity:

1) the fixed energy section, which accelerates ions from 5 MeV/u to 30 MeV/u;

2) the bent section, which boosts the energy up to 100 MeV/u;

3) the energy modulated section, that can provide beams in the variable-energy range, between 100 MeV/u and 430 MeVu. The energy modulation allows scanning the full depth of the tumour.

4.1.1 Fixed energy section

The fixed-energy section of the machine is designed to accelerate ions from 5 MeV/u up to 30 MeV/u. Being the first accelerating structure after the RFQ, it has the critical role of managing the frequency jump from 750 MHz to 3 GHz. Such a change in frequency results in a reduction of a factor 4 in phase acceptance and, consequently, a factor 2 in energy acceptance if compared to a 750 MHz structure with the same accelerating field. Two possible solutions have been studied, one at 750 MHz in two different variants, and the second at 3 GHz, managing the frequency jump at different energies.

The first option analysed for the structure following the RFQ is a 750 MHz Drift Tube Linac (DTL). This kind of structure operates at the same frequency of the RFQ, allowing to manage the frequency jump at higher energies. The DTL was studied in both Alvarez and a Quasi-Alvarez configurations, which are presented below.

750 MHz Alvarez DTL

The 7 metres long linac (a schematic of the cell structure of an Alvarez DTL is shown in Figure 19) was designed considering a constant accelerating gradient of 7.5 MV/m. This value is going to be updated once the RF design of the 3 modules is completed. The focusing lattice consists of 99 Permanent Magnetic Quadrupoles (PMQ) of the same length. The maximum gradient was chosen to be below the threshold of 400 T/m, corresponding to a maximum tip field of 1 T. This field value is considered the technological limit for permanent magnets. Due to this limitation, a FFDD focusing scheme has been chosen that allows for lower gradients than a conventional FD lattice.

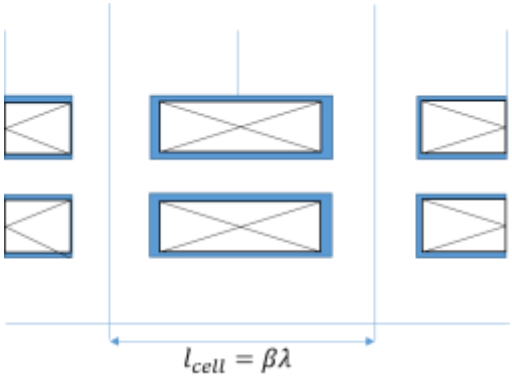

Figure 19: Alvarez DTL cell sketch.

As aforementioned, the linac is operated at the same frequency of the RFQ, making the injection process and the matching between the two structures easier than for a 3 GHz structure. As a drawback, the lower frequency results in a longer and bigger structure with a quadrupole per accelerating gap, increasing the overall production cost.

750 MHz Quasi-Alvarez DTL

The Quasi-Alvarez (QA) structure is a modified DTL with the FODO lattice in which the distance between RF gaps around each magnet is 2βλ. The QA can be designed in several configurations as shown in **Figure 20**. There is a long drift tube every $n\beta\lambda$ where n is the periodicity factor. Therefore, using a QA structure allows for longer quadrupoles and a longer FD lattice period length. Therefore, a conventional FD focusing lattice can be used with lower gradients. In addition, the drift tubes without magnets are designed with smaller dimensions and this leads to an increase of the effective shunt impedance (ZT^2), which represents the efficiency of the structure in converting RF power into accelerating gradient.

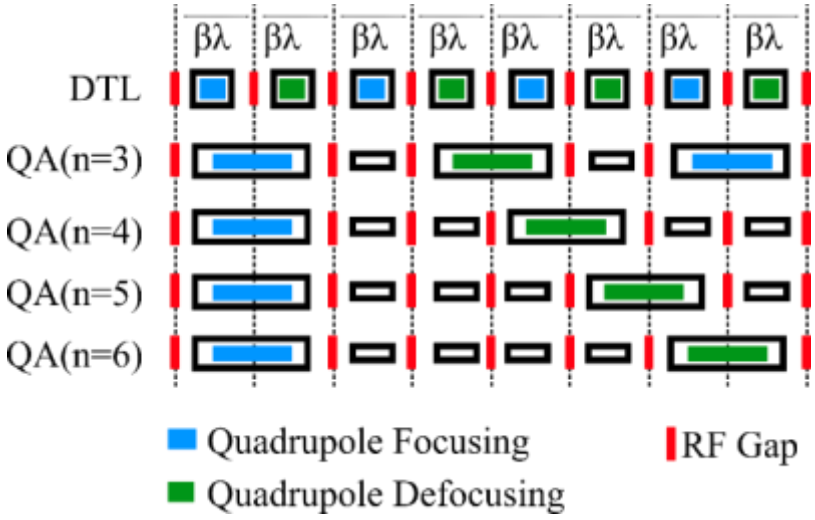

Figure 20: A schematic illustration of the QA.

A full QA tank can be considered as a series of sequential super-periods. In our design, the periodicity factor n is set to 4. In each super-period, one cell with the length of βλ is sandwiched between two 1.5βλ cells, as presented in **Figure 21**. As a drawback, the overall length of the linac is 7.5 m. This structure is also operated at 750 MHz, allowing, as the Alvarez DTL, for easy bunch-to-bucket injection from the RFQ. Moving the frequency jump from 5 MeV/u to 30 MeV/u makes the transition at 5 MeV/u easier. However, at 30 MeV/u the beam is much more rigid, making the longitudinal matching between the 750 MHz and 3 GHz more difficult.

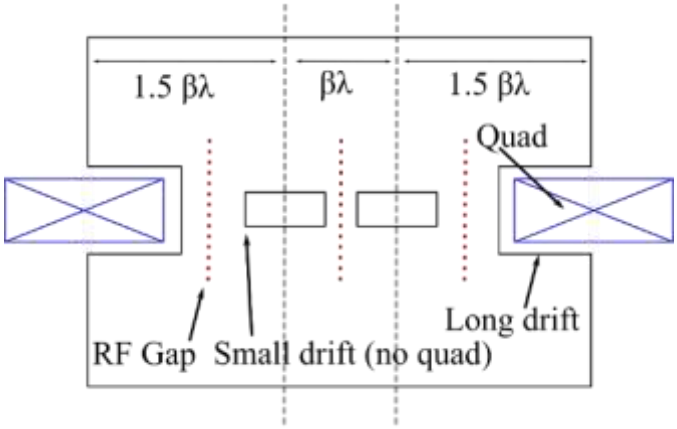

Figure 21: A schematic illustration of the Quasi-Alvarez super-period. The entire structure is designed by combining a set of these super-periods.

3 GHz Side Coupled Drift Tube Linac

The third structure considered for this section is a 3 GHz Side Coupled Drift Tube Linac (SCDTL), which is schematically described in **Figure 22**. Due to the high frequency, the drift tubes are not big enough to host the quadrupoles. Therefore, the quadrupoles are installed in between tanks, which are electro-magnetically coupled off axis.

The SCDTL structure was chosen for the LIGHT machine for proton therapy, designed and build by AVO/ADAM company [50]. The commissioning of such a machine demonstrated its capability of capturing and accelerating the beam from the 750 MHz RFQ.

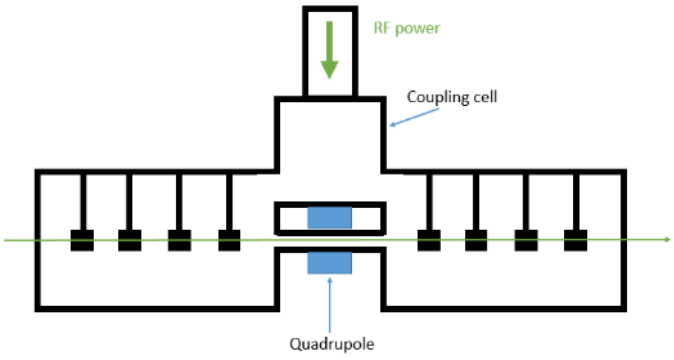

Figure 22: Side Coupled Drift Tube Linac structure schematic.

In this configuration, the frequency jump is managed at 5 MeV/u. Although, as a result, the longitudinal emittance experiences a 30% growth along the structure due to the difficult matching, the beam dynamics in the bent section becomes much easier to manage.

Unlike for the 750 MHz structure, the accelerating gradient is increased linearly with the beam energy in order to maximize the efficiency.

The main parameters of the three considered structures for the fixed-energy section are reported in **Table 6**.

Table 6: Comparison of the parameters of possible structures considered for the fixed energy section.

	Alvarez DTL	Quasi Alvarez DTL	SCDTL
Frequency [MHz]	750	750	3000
Length [m]	7	7.5	4.9
Energy [MeV/u]	5-30	5-30	5-30
E0T [MV/m]	7.5	7.5	12-23
Focusing pattern	FFDD	FD	FD
N quads	99	34	32
Max G [T/m]	400	200	300
L quad [mm]	20.4	60	50
N cells	99	102	177
N tanks	3	-	32
Transmission [%]	100	100	100

4.1.2 Bent section

The bent section of the linac was designed to cover a 180^0 angle minimizing as much as possible the effect of the bending magnets on the beam stability. In order to achieve this goal, a new beam dynamics scheme was developed that considers a configuration integrating accelerating tanks and bending magnets into a FD focusing scheme.

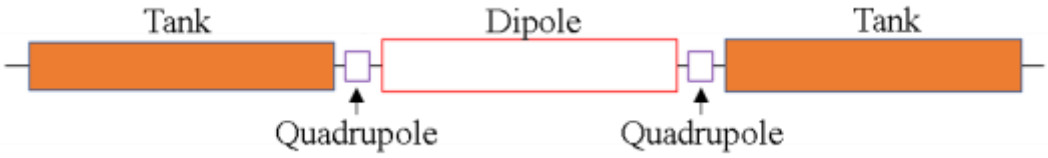

Figure 23: Schematic of the interlaced accelerating-bending configuration.

A schematic of a module of the bending section is shown in Figure 23. The length of the dipole is chosen to keep a constant transverse phase advance along the bent section. The magnetic field of the dipoles is the same for all magnets and equal to 1 T. Despite higher magnetic fields (1.6 T) that can be achieved with electromagnetic magnets, the field was set to 1 T to keep open the possibility of using permanent dipoles. This would result in a simpler operation and a lower power consumption.

Cell Coupled Linac structures at 3 GHz were chosen for acceleration in this section, which are operated in π-mode, allowing for shorter structures.

Every time that the beam travels into a dipole it experiences a drift in the longitudinal plane. Alternating dipoles and cavities, the beam can be re-bunched after every dipole, preventing losses.

Table 7: Main characteristics of the bent section.

Parameter	Value
Frequency [MHz]	3000
Length [m]	18
Energy [MeV/u]	30-100
E0T [MV/m]	20
Focusing pattern	FD
N quads	72
Max G [T/m]	300
L quad [mm]	50
N tanks	36
Transmission [%]	100
Transv. emit. Growth [%]	0
Long. Emit. Growth [%]	0

4.1.3 Energy modulated section

The energy modulation, required for longitudinal painting of the tumour, is achieved in this section of the linac by switching on and off the power into the accelerating cavities. The main issue related to the energy modulation is the beam transverse focusing. Changing the energy of the beam, in fact, the beam rigidity is changed, affecting the stability of the focusing channel. Thus, a quadrupole configuration and a set of input Twiss parameters, that lead to a perfect matching for one energy, will be mismatched for another energy. Despite this physical limitation, a PMQ settings configuration that guarantees a 100% transmission, zero emittance growth and a small beam size for all energies can be found.

The accelerating gradient E0T is increased to 30 MV/m and the synchronous phase ramped from -20 degrees (same as in the bent section) up to -15^0. Both choices are made in order to make the structure as compact as possible.

The energy-modulated section was designed, as the rest of the machine, considering permanent quadrupoles. Unlike the fixed-energy section and the bent section, the energy-modulated section is required to transport beams in the full range between 100 MeV/u and 430 MeV/u, thus changing the beam rigidity. The transverse phase advance law along the structure has therefore to be chosen carefully. The main characteristics of the energy-modulated section are summarized in Table 8.

Table 8: Main characteristics of the energy-modulated section.

Parameter	Value
Frequency [MHz]	3000
Length [m]	35
Energy [MeV/u]	100/430
E0T [MV/m]	30
Focusing pattern	FD
N quads	51
Max G [T/m]	230
L quad [mm]	50

N tanks	51
Transmission [%]	100

4.1.4 End-to-end tracking

The results shown so far are obtained considering the three sections of the linac as standalone structures. A free space between each part of the machine (set to 50 cm) is left with a double purpose; on one hand to accommodate the quadrupoles needed for the beam matching between the three sections and on the other to host beam instrumentation (beam position monitors, beam current transformers, etc.) and corrective elements (steerers, correctors, etc.). The matching section was designed to integrate the different sections of the machine.

To validate the linac design, an end-to-end tracking was performed from the source to the very end of the linac, including the matching sections, for the two final energies of 100 MeV/u and 430 MeV/u.

Table 9 shows the beam energy and emittances at the end of each section of the linac.

Table 9: Beam parameters at the end of each section of the linac resulting from tracking.

	Energy [MeV/u]	$\varepsilon_{x\text{-}x'}$ RMS norm. [π mm mrad]	$\varepsilon_{y\text{-}y'}$ RMS norm. [π mm mrad]	$\varepsilon_{\varphi\text{-}W}$ RMS norm. [π deg MeV]
TwinEBIS+LEBT	0.0015	0.026	0.0264	Continuous
RFQ	3	0.0271	0.027	0.431
Fixed energy section	30	0.028	0.0268	0.5958
Bent section	100	0.0279	0.0268	0.6277
Energy modulated section	100	0.0284	0.0269	0.6222
Energy modulated section	430	0.0279	0.0268	0.623

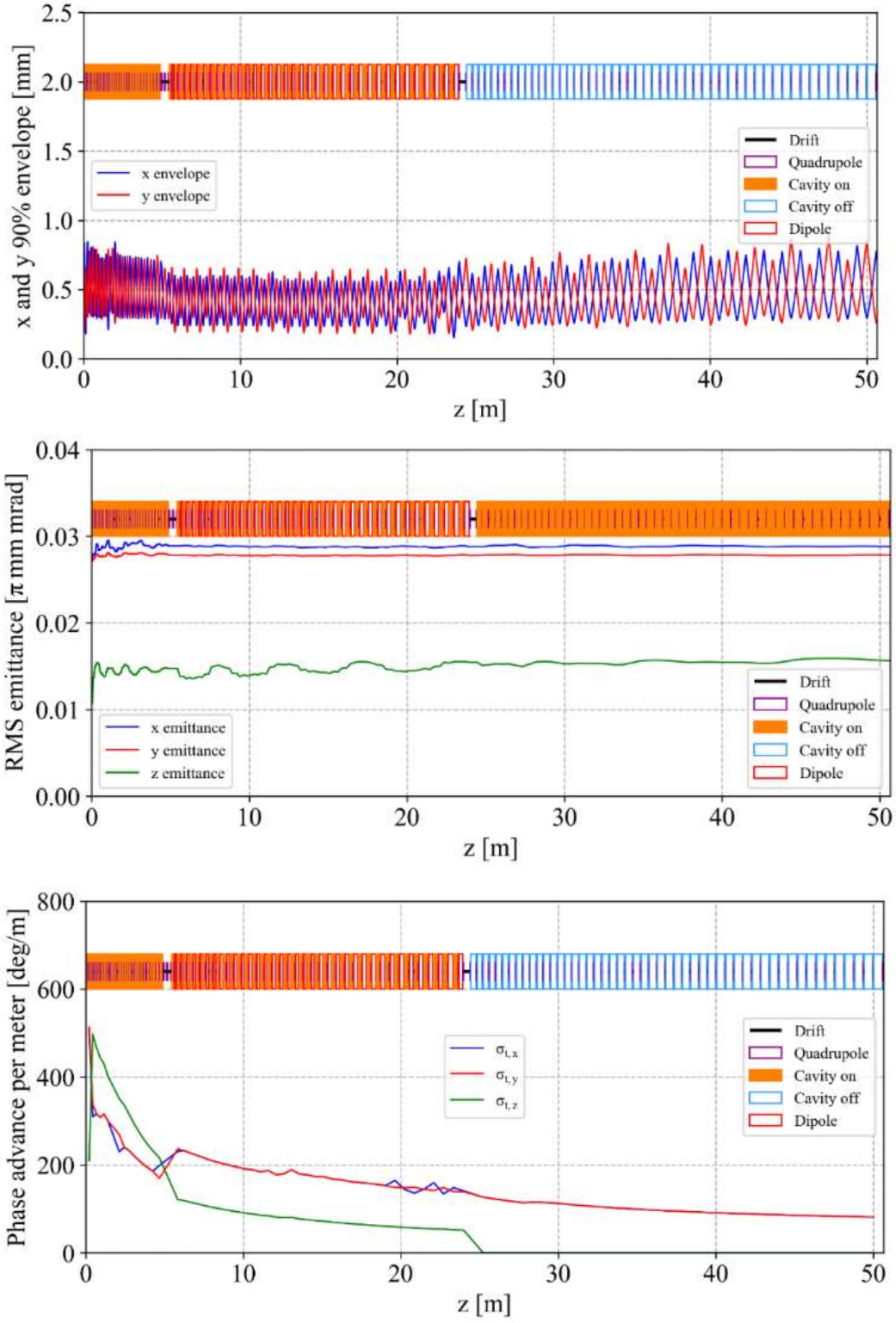

Figure 24: Beam envelopes, emittances and transverse phase advance resulting from the end-to-end tracking with a final energy of 100 MeV/u.

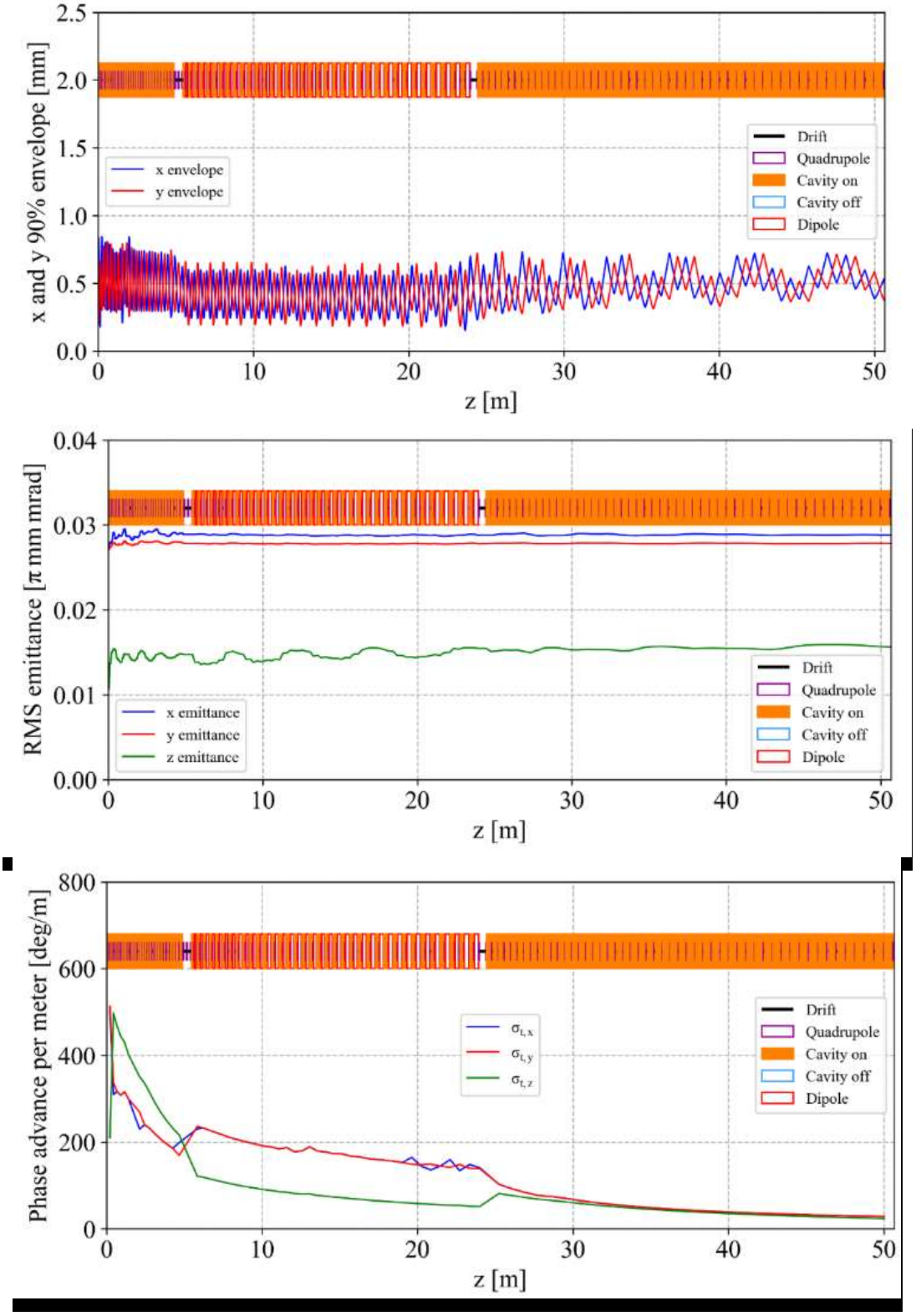

Figure 25: Beam envelopes, emittances and transverse phase advance resulting from the end-to-end tracking with a final energy of 430 MeV/u.

4.2 Alternatives for the fixed energy section, detailed RF design

Several structures have been proposed for the fixed-energy section, as discussed earlier. The DTL can provide sufficient strong focusing and consequently higher longitudinal and transverse beam transmission; however, housing PMQs inside drift tubes is challenging because of the small dimension of the drift tubes at lower energies at 750 MHz. The SCDTL structure is very efficient and leaves space for the quadrupoles, but for the low energies of carbon-ion beams the length of its cells is much smaller than for the structures built for protons, and its mechanical and RF feasibility is not guaranteed. The Quasi Alvarez DTL is a valid alternative in terms of efficiency, cost, and mechanical feasibility, but because no examples exist of 750 MHz Quasi-Alvarez, its design has to be further developed and compared to the other alternatives. The first QA tank, after the RFQ, is the most critical because of the shortest cell length, and has been analysed in detail.

The first Quasi-Alvarez tank is designed to accelerate a beam of C^{6+} particles from 5 MeV/u to 7 MeV/u. The RF design is performed by maximizing the effective shunt impedance as well as bringing mechanical and physical constraints within the limit. The maximum electric field at surfaces needs to be kept below the breakdown threshold that is 38 MV/m in our design. In addition, the dimension of stems and drift tube needs to be optimized to make sure that the cooling circuit and PMQ can be embedded inside. The Quasi-Alvarez tank is designed for the different axial accelerating gradient of 4 MV/m and 8 MV/m, in order to compare costs related to the RF power sources. Both cases are studied initially using 2D models and considering axial symmetry conditions. Further studies on power loss on stems are performed using 3D models. The main RF parameters of both structures are listed in **Table 10**. The 3D plot of the Tank at 4 MV/m is shown in Figure 26.

Table 10: Main parameters of Quasi-Alvarez structure at the axial accelerating gradients of 4 MV/m and 8 MV/m.

	4 MV/m	8 MV/m
Frequency [MHz]	750	750
Length [m]	1.63	0.89
Energy [MeV/u]	5-7	5-7
Peak current [mA]	0.2	0.2
Peak power [kW]	0.19	0.59
N cells	27	15
N quads	8	4
Max. Surface E-field [MV/m]	23	35

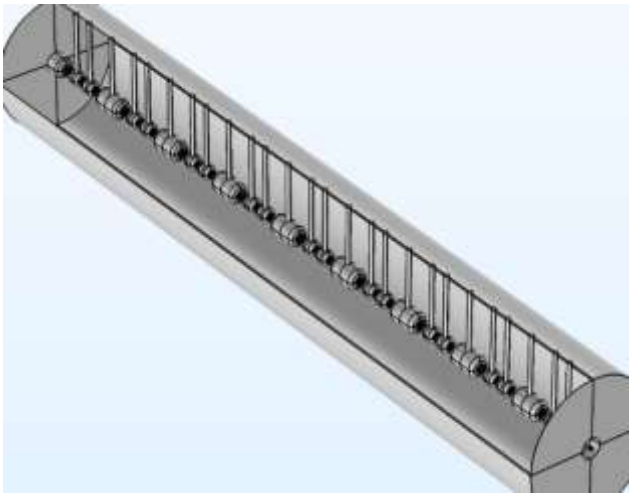

Figure 26: Quasi-Alvarez geometry at 4 MV/m.

5. Required R&D and risk comparison

To compare the three options under study for SEEIIST, a first element to be considered is the amount of R&D needed before implementation, which has an impact on the timeline of the project, its cost, and its risk level.

5.1 Warm magnet synchrotron at higher beam intensity

Medical synchrotrons, based on normal conducting magnets, are well known and the risk associated with this technology is low. However, the advanced warm synchrotron development has to focus on improving the injection to reach such a record stored intensity of 2 10^{10} Carbon-ions per cycle, by improving:

- the source, to increase the ion intensity (in the same beam emittance);
- the injector linac, to improve transmission;
- the multiturn injection process.

Moreover, handling of the multi-energy flat-tops for slow extraction also requires development, and the system needs to stay flexible to the possible new dose-delivery requirements.

The increase in the ion-source current is considered as relatively low-risk, suitable designs being already close to market. Improving the linac transmission might be more critical; however, new linac designs and more modern beam optics simulations tools have a strong potential in leading to higher transmission. The R&D for multi-turn injection consists mainly in simulations.

Altogether, the level of R&D required to build a warm-magnet synchrotron configuration at increased beam intensity is low. The only component requiring both simulation studies and prototyping is the linac, with the construction of another copy of the standard injector being a straightforward mitigation in case of problems related with this R&D.

5.2 Superconducting synchrotron

The compact super-conducting synchrotron, in addition to the same R&D needed for the warm-magnet synchrotron, has the novelty of the magnet technology.

- The development and construction of 90^0 curved magnets with a radius of curvature of about 2 m is challenging. Simulations and testing are required, and a prototype is needed before industrialisation. In case 90^0 is not feasible, the backup option is to split the magnets in units of 45^0 or 30^0.
- Reaching a ramp-rate of up to 1 T/s requires R&D and care in the dimensioning of the heat-load due to eddy-currents and other dynamics effects. The prototype should also address this point. In any case, even if the ramp-rate were only 0.10 T/s, resulting in a total cycle length of about 1 minute, this would be justified if the entire dose is delivered in one cycle.
- Detailed beam-dynamic modelling of these special magnets must be done, and field maps compared versus theory and measurements in the prototype.

The R&D needed to design and prototype these magnets requires a considerable investment in terms of budget and personnel resources, and a time span of about 5 years. Some European research institutions are already starting R&D programmes on curved pulsed superconducting magnets for small synchrotrons and a wide collaboration in this research direction will provide the required resources and expertise. The risk of this development is considered as medium, because mitigations in case of problems exist (magnets with small bending angle), but they might spoil the cost effectiveness of the superconducting solution brining the cost of the magnets at the same level as the warm-magnet option.

5.3 Full linac

Finally, the design of the full-linac solution is very advanced, however, since it is novel, there are many items and hardware, which still require R&D:

- the C^{6+} EBIS source is presently in prototyping phase at CERN. Its performance has to be assessed and optimised.

- the 750 MHz RFQ for Carbon is 5 m long, 66% longer than the 3 m-long proton version built at CERN for the ADAM company. Specific solutions for reaching the required longitudinal field symmetry in this configuration have to be developed and tested, possibly on a prototype.
- the SCDTL, Alvarez DTL or Quasi-Alvarez DTL structures after the RFQ have to be completely designed (RF resonator, mechanical structure) starting from the beam optics layout presented in this report. This requires a series of radio-frequency simulations integrated with the mechanical design and the construction and testing of a prototype.
- the PMQs require prototyping and optimisation because of their reduced dimensions. The small aperture makes beam alignment particularly challenging and requires a sophisticated concept for beam diagnostics and steering that has to be defined.
- Finally, one of the cost drivers for the linac is the high-power radio-frequency system. Conventional 3 GHz klystrons exist on the market, but, because of their relatively low power and large number, their impact on the cost of the linac is substantial. A solution to reduce the cost is to use Multi-Beam Klystrons (MBK) that are still in the development phase by a Russian company. The cost, reliability, and feasibility of MBK's need to be assessed with the aim of reducing the construction cost of the full linac.

The time to complete the R&D for a full-linac option is estimated of the order of 5-7 years, if sufficient resources are available. The risk for this option is considered as medium.

6. Facility layout and dimension comparison

The optimised accelerator designs identified in the previous sections have been integrated in an overall facility design, using the configuration of beam lines and treatment/experimental rooms defined in [31]. For the shielding walls, thicknesses of similar values as for the existing ion therapy facilities were adopted, waiting for precise radiation protection calculations. In the case of the synchrotrons, the ion sources and the injector linac are external to the main accelerator area to allow access during operation.

The facility layout for the three considered options, i.e. the (a) warm-magnet synchrotron, (b) super-conducting magnet synchrotron and (c) full-linac complex are shown in **Figure 27**, **Figure 28** and **Figure 29** respectively. The corresponding dimensions of their main accelerator areas are:

(a) for the normal conducting ring: about 900 m^2 adding up to about 1200 m^2 including the source plus injector linac areas (inner dimensions);

(b) for the superconducting ring: about 360 m^2 adding up to 600 m^2 including the source plus injector linac areas (inner dimensions), which can be further optimized;

(c) for the full-linac option about 600 m^2 including, by default, the source and injector linac in the same area (inner dimensions).

Both, the superconducting-magnet and the full-linac options occupy a similar surface, which is smaller than the one occupied by the warm synchrotron (by about 600 m^2), corresponding to a 50% reduction in footprint. The surface of the overall facility including beam transport, treatment and experimental rooms is (a) 6500 m^2 for the normal-conducting (b) 5500 m^2 for the super-conducting and (c) 5550 m^2 for the full-linac options. Hence, compared to the surface occupied by the warm-synchrotron complex the other two layouts require, both, a smaller area by 1000 m^2 corresponding to a 15% reduction in footprint.

Considering only the accelerator part, the superconducting ring is definitely smaller than other options, and further reductions could come from additional optimizations. However, the advantage of this solution is more pronounced for small centres with only a few treatment rooms, while for configurations with a large number of treatment or experimental rooms requiring a complex beam distribution the difference is smaller. SEEIIST as a large centre for research and therapy is presently conceived with five beam lines, and, in this case, a reduced accelerator complex footprint brings limited advantage. In fact, the three treatment rooms, the two experimental areas, the HEBT area, and the main service area, that are the same for all options, occupy some 4500 m^2.

The bent-linac configuration, fitting in 30 m x 10 m room, allows hosting a 50 m long linac in a standard building. In this solution, however, contrary to what is foreseen for the two synchrotrons, the source and the RFQ are in the main accelerator area, and thus they are not accessible for tuning or maintenance during operation.

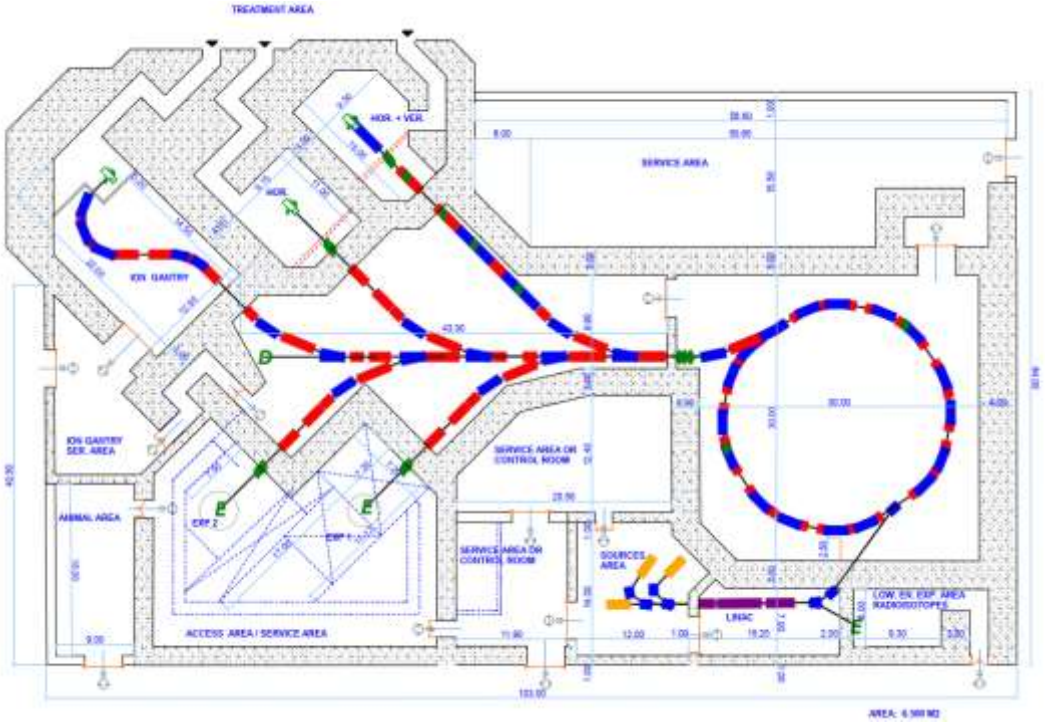

Figure 27: The layout of the accelerator's area, based on the 25-meter diameter warm synchrotron.

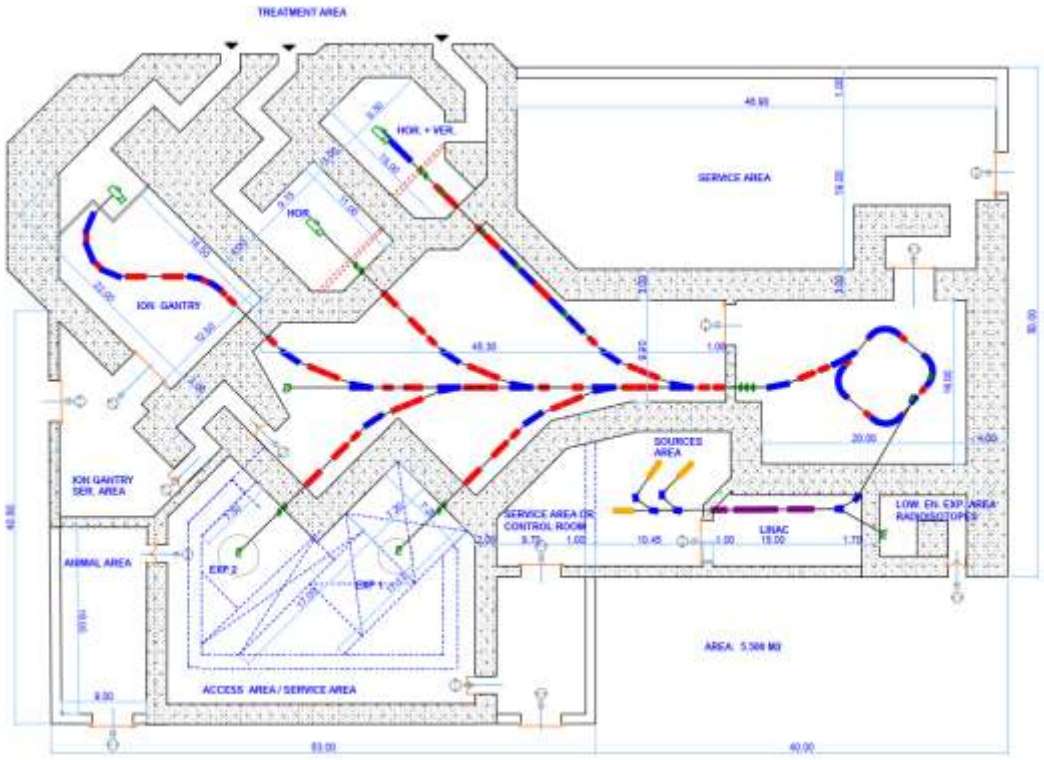

Figure 28: The layout of the accelerator's area, based on a compact super-conducting synchrotron.

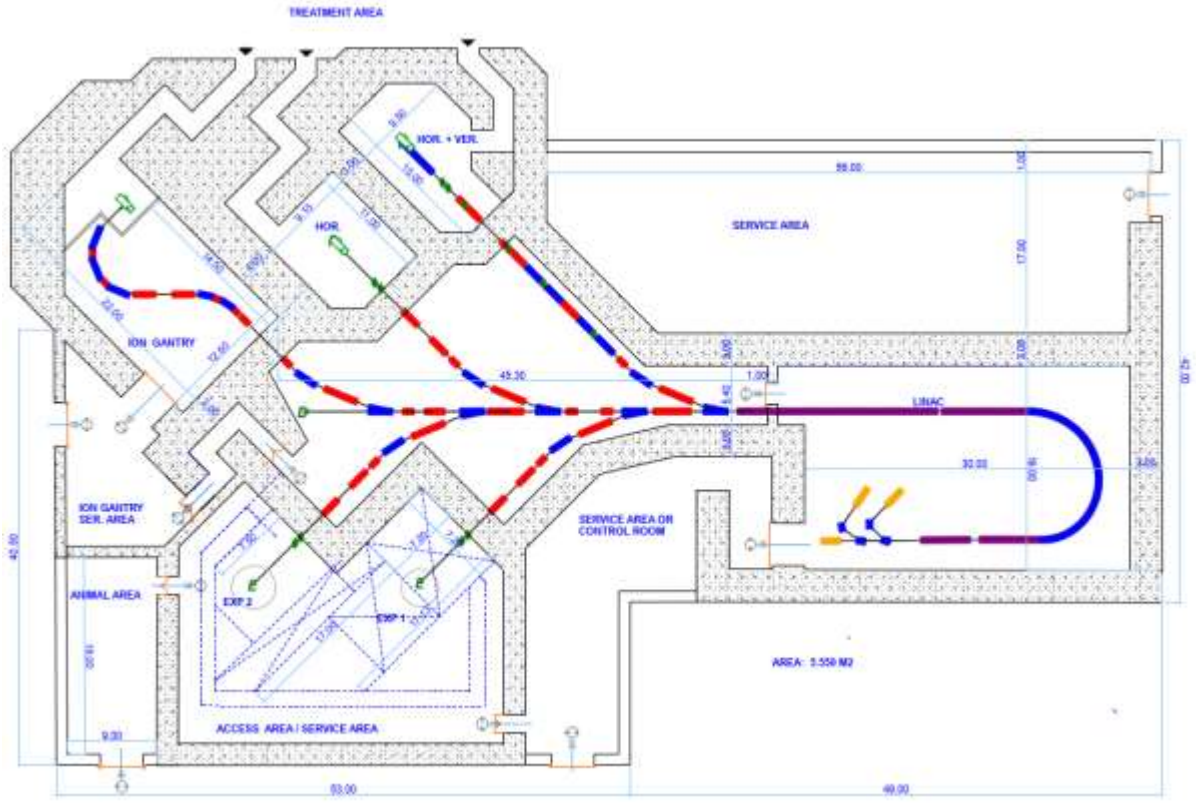

Figure 29: The layout of the facility's area based on the full-linac option.

7. Cost comparison

The cost of the three options has been compared, trying to define a homogeneous set of data starting from the warm synchrotron, for which precise construction estimates are available. In all cases, only the cost up to the extraction from the accelerator is considered, the costs for beam transport lines and for beam delivery being approximately the same for all options.

High energy beam lines, medical systems and controls, not included since they are similar for all three options, account for an additional 33 MEUR.

Civil engineering and infrastructure (e.g. electrical distribution, cooling and ventilation) costs are not included in the comparison. They have been estimated for the PIMMS-type layout presented in [5] in 45 MEUR.

7.1 Warm-magnet synchrotron

For the warm-magnets synchrotron option, a precise estimate of the costs has been done for the SEEIIST Report [7], in collaboration with CNAO. The additional features foreseen in the present design, with respect to the standard PIMMS, are not expected to have a large impact on the cost. **Table 11** presents the numbers from the Report and the percentage with respect to the total cost. Since estimates were done in 2017, an increase by 10% should be included in the estimate. The magnets and power supplies are the main cost drivers, followed by the injector linac. This is the reason behind the decision to revise the injector linac design and to optimize the number of magnets.

The cost of the synchrotron including the injector is of 42 MEUR.

The estimated construction cost of the entire facility is 120 MEUR, with operating costs for the accelerator part estimated at 11 MEUR/year.

Table 11: Cost of the warm magnet synchrotron.

Main elements	**Cost in kEUR**	
3 Sources	4'800	11%
Linac	10'700	25%
Magnets	11'900	28%
Power Supplies	8'600	20%
RF system	600	1%
Beam diagnostics	4'700	11%
Vacuum	700	2%
total =	42'000	100%

7.2 Superconducting synchrotron

Starting from these numbers, it is possible to estimate the cost of the superconducting option (**Table 12**), which has the same injector linac and sources, a similar RF system and injection/extraction hardware.

Table 12: Cost of the superconducting synchrotron.

Main elements	**Cost in kEUR**	
3 Sources	4'800	16 %
Linac	10'700	35 %
Magnets (normal conducting)	1’300	4 %
Power Supplies	1’800	6 %
SC magnets	3’500	11 %
machining tools	1’000	3 %
Cryostat and cryocoolers	2’500	8 %
RF system	600	2 %
Beam diagnostics	4'500	15 %
Vacuum	240	1 %
total =	30'940	100%

The beam instrumentation is comparable, only the number of beam-position monitors will be smaller. The vacuum can be scaled with the circumference length. Moreover, the superconducting synchrotron will have 8 small quadrupoles, 8 correctors and 5 sextupoles. Concerning the superconducting magnets, they represent the most delicate R&D items. In addition to the cost of the material, i.e. the Nb-Ti superconductor, that is not very expensive (200 kEUR per magnet), the shielding iron (150 kEUR per magnet) and the structural elements including the manufacturing process (350 kEUR per magnet), the cost of the manufacturing tools should be considered, which is an one-time expense of 1 MEUR, and the cryogenics. If other magnets for additional accelerators are built, their cost per unit will decrease. For the purpose of this exercise, however, we assume that only the 4 magnets of the ring plus 1 extra spare magnet, which can be used for the magnetic field reference, are built.

The estimated total cost for the superconducting synchrotron option is about 31 MEUR. Operating costs are expected to be lower.

7.3 Full-linac

Concerning the full-linac option, an approximate cost estimate has been performed and is reported in Table 13, giving as a result about 31 MEUR, i.e. the same as the superconducting synchrotron option.

Table 13: Cost of the full-linac option.

Main elements	**# of elements**	**Cost / element**	**total cost in kEUR**
ion source+LEBT	1	0.7	700
RFQ – per meter (all included)	4	1	4'000
750 MHz ICH (**up to 10 MeV/u**)			
* Cavity 1 – per meter	0.33	250	82.5
* Cavity 2 – per meter	0.38	250	95
* Cavity 3 – per meter	0.82	250	205
* Cavity 4 – per meter	0.98	250	245
* RF - IOT	3	100	300
3 GHz DTL (up to 100 MeV/u)			
* Module (x5 modules)	5	500	2'500
Transport (180 deg bend)			
* bending magnets	2	100	200
3 GHz HE CCL (**up to 430 MeV/u**)			
* Cavities (vacuum, RF included)	32	500	16'000
Instrumentation	65	100	6'500
total =			30'828

8. Conclusions: accelerator comparison and recommendations for SEEIIST

The following **Table 14** summarizes and compares the advantages and disadvantages of the three accelerator solutions that have been analysed in detail in the previous sections.

Table 14: Comparison of the three accelerator options.

	Construction Cost	Operation cost	Footprint	Performance	Time to development	Risk of development	Treatment protocols	Gantry
Warm (new) synchrotron	Medium	Medium	Large	Good	Low	Low	Existing	Simple design
Superconducting synchrotron	Lower	Lower	Small	Good	Medium	Medium	Existing	Simple design
Linear accelerator	Lower	Lower	Small	Better	Long	Medium	To be developed	Complex design

The main advantages of the linac, as compared to other types of particle therapy accelerators, are the fast beam delivery (the linac beam being pulsed at 200 Hz frequency) and the corresponding fast pulse-to-pulse modulation of the energy. However, these advantages have also setbacks because standard gantry designs are not compatible with the fast energy variation, requiring a new gantry design with large acceptance, and because all treatment protocols will have to be reassessed for the linac operating mode, lengthening the time and costs of the licensing phase. It is considered that the required developments will need many years before an ion linac can be used to treat patients. The cost of a linac is dominated by the radio-frequency generation system, and the key to controlling the cost is using multi-beam klystrons that are still under

development. In terms of footprint, the linac presents an advantage with respect to a conventional synchrotron, which becomes much more pronounced if the linac is "folded", integrating a 180^0 bending section that would reduce the footprint but can considerably increase the cost.

An additional limitation of the full linac is that it is designed for a q/m ratio 1/2, i.e. it can accelerate only fully stripped carbon or helium (plus of course protons). It is an interesting solution for hospitals, however, it might not be suitable for SEEIIST, which has a rich research program with different ions. On the contrary, the injector linac for the synchrotrons is designed for q/m = 1/3 and is capable of accelerating other ion species (partially stripped carbon, oxygen, etc.).

The superconducting synchrotron is the most compact of the three options and its construction cost is lower than for a conventional synchrotron because of the smaller amount of components, the relatively low cost of the superconducting magnets using standard Nb-Ti conductor, and some reduction in the cost of civil engineering. The energy of the beam can be modulated during the pulse, and the long rise and fall times of the superconducting magnet ramp are not considered a limitation. Europe has a leadership position in the development and construction of superconducting magnets for accelerators and has a large set of companies that can produce superconducting cables and full magnets of any design. However, curved magnets are challenging and the CCT coil configuration needs extensive R&D and prototyping, before it can become standard. The design is still to be fully developed and the compact dimensions, together with the high rigidity of carbon ions makes its development challenging. The magnet technology represents the main risk. Since SEEIIST should start construction as soon as possible, this technology is considered not mature yet.

A warm-magnet synchrotron with novel beam delivery schemes and a factor 20 higher intensity (by design) compared to European facilities represents the more adequate option for SEEIIST, assuming that construction can already start as early as 2023, despite the larger footprint and cost of the facility.

In case the time for construction stretches, it would become interesting to look at the superconducting option, as first and novel accelerator of this kind. Moreover, since the injector linac is the same for both options, and the bunker similar, one could start with the construction of the injector linac and postpone the choice of the ring, allowing for further progress with the synchrotron design.

This study recommends to SEEIIST the adoption as baseline configuration of a warm-magnet synchrotron accelerator with novel features. Development of superconducting magnets and adequate superconducting synchrotron designs should continue as an advanced alternative option. The superconducting alternative with its potentially lower cost and smaller dimensions might become the baseline in case the preparation for construction of SEEIIST would take more time than foreseen and in case of success of the superconducting magnet development. Additionally, the superconducting option might more easily become a standard commercial design for a next generation of ion therapy facilities beyond SEEIIST.

9. List of acronyms

AG-CTT	Alternating Gradient Canted Cosine Theta
BNL	Brookhaven National Laboratory
CERN	Conseil Européen pour la Recherche Nucléaire
CNAO	Centro Nazionale Adroterapia Oncologica
DBA	Double-Bend Achromat
DTL	Drift-Tube Linac
EBIS	Electron-Beam Ion Source
ECR	Electron Cyclotron-Resonance
FFA	Fixed Field Alternating gradient
HIT	Heidelberg Ion Therapy center
HT	Hadron Therapy
INFN	Istituto Nazionale Di Fisica Nucleare
LET	Linear Energy Transfer
LLRF	Low Level Radio Frequency
MIT	Marburg Ion-beam Therapy
NIRS	National Institute for Radiological Sciences
PAMELA	Particle Accelerator for Medical Applications
PIMMS	Proton-Ion Medical Machine Study
PMQ	Permanent Magnetic Quadrupoles
QA	Quasi-Alvarez
RBE	Relative Biological Effectiveness
RF	Radio Frequency
RT	Radiotherapy
RF-KO	Radio Frequency-Knock Out
RFQ	Radio Frequency Quadrupole
SCDTL	Side Coupled Drift Tube Linac
SEEIIST	South East European International Institute for Sustainable Technologies
TERA	TErapia con Radiazioni Adroniche (Foundation)

10. References

[1] R. Wilson, "Radiological use of fast protons," *Radiology,* p. 47(5):487–91, 1946.

[2] Nuclear Physics for Medicine, Nupecc book, 2014, p. 41.

[3] "PTCOG: Particle Therapy Co-Operative Group," 2020. [Online]. Available: https://www.ptcog.ch/.

[4] T. Okada, T. Kamada, H. Tsuji, J.-e. Mizoe, M. Baba, S. Kato, S. Yamada, S. Sugahara, S. Yasuda, N. Yamamoto, R. Imai, A. Hasegawa, H. Imada, H. Kiyohara, K. Jingu, M. Shinoto and H. Tsujii, "Carbon Ion Radiotherapy: Clinical Experiences at National Institute of Radiological Science (NIRS)," *Journal of Radiation Research,* vol. 51, pp. 355-364, 5 2010.

[5] HIT web-page, [Online]. Available: www.hit-heidelberg.com.

[6] Kopp, B., et al., "Development and Validation of Single Field Multi-Ion Particle Therapy Treatments," *International Journal of Radiation Oncology,* vol. 106, no. 1, pp. 194-205, 2020.

[7] Amaldi, U., et al., "A facility for tumour therapy and biomedical research in South-Eastern Europe," CERN-2019-002, 2019.

[8] V. Lazarev et al., "Technical overview of the Siemens Particle Therapy accelerator," in *IPAC2011,* San Sebastian, Spain, 2011.

[9] MIT web-page, [Online]. Available: https://www.mit-marburg.de/.

[10] P. J. Bryant, L. Badano, M. Benedikt, M. Crescenti, P. Holy, A. T. Maier, M. Pullia, S. Reimoser, S. Rossi, G. Borri, P. Knaus, F. Gramatica, M. Pavlovic and L. Weisser, "Proton-Ion Medical Machine Study (PIMMS), 2," CERN, 2000.

[11] CNAO web-page, [Online]. Available: www.fondazionecnao.it.

[12] MedAustron web-page, [Online]. Available: www.medaustron.at.

[13] ARIES web-page, [Online]. Available: https://aries.web.cern.ch/home.

[14] https://indico.cern.ch/event/682210/overview, *Ideas and technologies for a next generation facility for medical research and therapy with ions,* Archamps: European Scientific Institute, 2018.

[15] E. Benedetto, N. Al Harbi, L. Brouwer, S. Prestemon, P. Riboni and U. Amaldi, "A carbon ion superconducting gantry and a synchrotron based on Canted Cosine Theta magnets," *Submitted to: Physics in Medicine and Biology,* 2020.

[16] V. Bencini, Design of a novel linear accelerator for carbon ion therapy, Geneva: CERN-THESIS, 2019.

[17] S. Benedetti, A. Grudiev and A. Latina, "High gradient linac for proton therapy," *Phys. Rev. Accel. Beams,* vol. 20, no. 4, p. 040101, 2017.

[18] Trobojevic, D., et al., "Lattice Design of a Rapid Cycling Medical Synchrotron for Carbon/Proton Therapy," in *IPAC2011,* 2011.

[19] Peach, K., et al., "Conceptual design of a nonscaling fixed field alternating gradient accelerator for protons and carbon ions for charged particle therapy," *Phys. Rev. ST Accel. Beams,* vol. 16, no. 3, p. 030101, 2013.

[20] Jongen, Y., et al., "IBA C400 Cyclotron Project For Hadron Therapy," 2007.

[21] Jongen, Y., et al., “Compact superconducting cyclotron C400 for hadron therapy,” *Nuclear Instruments and Methods in Physics Research Section A: Accelerators, Spectrometers, Detectors and Associated Equipment,,* vol. 624, no. 1, pp. 47-53, 2010.

[22] IBA press release, 20 Sept. 2019. [Online]. Available: https://iba-worldwide.com/content/iba-subsidiary-normandy-hadrontherapy-launches-development-carbon-therapy-system-normandy.

[23] Masood, U., Bussmann, M., Cowan, T.E. et al. , “A compact solution for ion beam therapy with laser accelerated protons,” *Appl. Phys. B,* vol. 117, p. 41–52 , 2014.

[24] Witte, H., et al., “The Advantages and Challenges of Helical Coils for Small Accelerators—A Case Study,” *IEEE Transactions on Applied Superconductivity,* vol. 22, no. 2, pp. 4100110-4100110, 2012.

[25] Y. Iwata, T. Kadowaki, H. Uchiyama, T. Fujimoto, E. Takada, T. Shirai, T. Furukawa, K. Mizushima, E. Takeshita, K. Katagiri, S. Sato, Y. Sano and K. Noda, “Multiple-energy operation with extended flattops at HIMAC,” *Nuclear Instruments and Methods in Physics Research Section A: Accelerators, Spectrometers, Detectors and Associated Equipment,* vol. 624, pp. 33-38, 2010.

[26] U. Amaldi, “Oblique raster scanning: an ion dose delivery procedure with variable energy layers,” *Phys. Med. Biol.,* vol. 64, p. 115003, 2019.

[27] U. Amaldi, “Lectures at the “Nuclear Technologies and Clinical Innovation in Radiation Oncology” Workshop,” Trento, 2011.

[28] Schmitzer, C, et al., “MedAustron Synchrotron RF Commissioning for Medical Proton Beams,” in *IPAC 2016,* Busan, Korea, 2016.

[29] Ohmori, C. et al., “Development of a high gradient rf system using a nanocrystalline soft magnetic alloy,” *Phys. Rev. Accel. Beams,* vol. 16, no. 11, p. 112002, 2013.

[30] Pauluzzi, M., et al., “The new 1-18 Mhz Wideband RF System for the CERN PS Booster,” Melbourne, 2019.

[31] Sapinski, M., et al., “Technical report on beam delivery for an ion therapy and research facility in SEE,” Deliverable 2.2: Service Contract "Advancing the Design of the South-East European International Institute for Sustainable Technologies (SEEIIST)" , 2020.

[32] A. Advic, “Multiturn injection of Carbon Ions in a Medical Synchrotron,” Master Thesis, 2020.

[33] B. Schlitt, "Commissioning and Operation of the Injector Linacs for HIT and CNAO," in *Proc. of Linear Accelerator Conference (LINAC'08), Victoria, British Columbia, Canada, Sep 29- Oct 3, 2008*, Geneva, 2008.

[34] Pantechnik, “Supernanogan,” March 2013. [Online]. Available: https://www.pantechnik.com/wp-content/uploads/2020/07/Supernanogan.pdf.

[35] Pantechnik, “PK-ISIS,” March 2013. [Online]. Available: https://www.pantechnik.com/wp-content/uploads/2020/07/PK-ISIS.pdf.

[36] Celona, L., et al., “Experimental characterization of the AISHa ion source,” *Review of Scientific Instruments,* vol. 90, no. 11, p. 113316, 2019.

[37] M. Breitenfeldt, R. Mertzig, J. Pitters, A. Shornikov and F. Wenander, “The TwinEBIS setup: Machine description,” *Nuclear Instruments and Methods in Physics Research Section A: Accelerators, Spectrometers, Detectors and Associated Equipment,* vol. 856, pp. 139-146, 2017.

[38] X. Zhang, “Lattice Design of a Carbon-Ion Synchrotron based on Double-Bend Achromat Lens,” 2020.

[39] A. Jackson, Particle Accelerators, 1986, pp. 22, 111.

[40] W. Hardt, “Ultraslow extraction out of LEAR (transverse aspects),” CERN Internal Note PS/DL/LEAR Note 81-6., 1981.

[41] Iwata, Y., et al., “Development of Carbon-Ion Radiotherapy Facilities at NIRS,” *IEEE Transactions on Applied Superconductivity,* vol. 28, no. 3, pp. 1-7, 2018.

[42] L. Brouwer, S. Caspi, R. Hafalia, A. Hodgkinson, S. Prestemon, D. Robin and W. Wan, “Design of an Achromatic Superconducting Magnet for a Proton Therapy Gantry,” *IEEE Trans. Appl. Supercond.,* vol. 27, no. 4, p. 44001006, 2016.

[43] D. Meyer and R. Flasck, “A new configuration for a dipole magnet for use in high energy physics applications,” *Nucl. Instr.Meth. Phys. Res. A,* vol. 80, no. 2, pp. 339-341, 1970.

[44] C. Goodzeit, M. Ball and R. Meinke, “The double-helix dipole - a novel approach to accelerator magnet design,” *IEEE Trans. Appl. Supercond.,* vol. 13, no. 2, p. 1365–1378, 2003.

[45] “MADX Users guide,” [Online]. Available: http://cern.ch/madx/releases/last-rel/madxuguide.pdf. [Accessed 2019].

[46] Y. Iwata, K. Noda, T. Murakami, T. Shirai, T. Furukawa, T. Fujita, S. Mori, S. Sato, K. Mizushima, K. Shouda, T. Fujimoto, H. Arai, T. Ogitsu, T. Obana, N. Amemiya, T. Orikasa, S. Takami and S. Takayama, “Development of a superconducting rotating-gantry for heavy-ion therapy,” *Journal of radiation research,* vol. 55 Suppl 1, pp. i24-i25, 3 2014.

[47] Amaldi, U., et al., “LIBO—A linac booster for proton therapy: Construction and test of a prototype,” *Elsevier Nuclear Instruments and Methods in Physics Research Section A: Accelerators, Spectrometers, Detectors and Associated Equipment,* vol. 521, no. 2-3, pp. 512-529, 2004.

[48] S. Andrés, U. Amaldi and A. Faus-Golfe, “CABOTO, a high-gradient linac for hadrontherapy. Journal of Radiation Research.,” *Journal of Radiation Research,* vol. 54, pp. i155-i161, 2013.

[49] Bencini, V., et al., “High Frequency RFQ Design and LEBT Matching for the CERN TwinEBIS Ion Source,” 2018.

[50] AVO/ADAM web-page, [Online]. Available: https://www.avoplc.com/en-gb/Technology/Overview-of-the-LIGHT-System.